REPORT DOCUMENTATION PAGE

1. AGENCY USE ONLY (Leave blank)	2. REPORT DATE	3. REPORT TYPE AND DATES COVERED
	5/20/96	Final Rpt. 4/19/95 - 11/30/97

4. TITLE AND SUBTITLE
Continuing Development of a "Hybrid" Model (VSH) of the Nautral Thermosphere"

5. FUNDING NUMBERS
NAS8-40578

IN-46-CR
2-17
162624

6. AUTHOR(S)
Dr. Alan Burns

NASA/CR-96- 206524

7. PERFORMING ORGANIZATION NAME(S) AND ADDRESS(ES)
The University of Michigan
Space Physics Research Laboratory
2245 Hayward St.
Ann Arbor, MI 48109-2143

8. PERFORMING ORGANIZATION REPORT NUMBER

9. SPONSORING/MONITORING AGENCY NAME(S) AND ADDRESS(ES)
NASA
George C. Marshall Space Flight Center
Marshall Space Flight Center, AL 35812

10. SPONSORING/MONITORING AGENCY REPORT NUMBER

11. SUPPLEMENTARY NOTES

12a. DISTRIBUTION/AVAILABILITY STATEMENT

12b. DISTRIBUTION CODE

13. ABSTRACT *(Maximum 200 words)*

We propose to continue the development of a new operational model of neutral thermospheric density, composition, temperatures and winds to improve current engineering environment definitions of the neutral thermosphere. This model will be based on simulations made with the National Center for Atmospheric Research (NCAR) Thermosphere-Ionosphere-Electrodynamic General Circulation Model (TIEGCM) and on empirical data. It will be capable of using real-time geophysical indices or data from ground-based and satellite inputs and provides neutral variables at specified locations and times. This "hybrid" model will be based on a Vector Spherical Harmonic (VSH) analysis technique developed (over the last 8 years) at the University of Michigan that permits the incorporation of the TIGCM outputs and data into the model. The VSH model will be a more accurate version of existing models of the neutral thermosphere, and will thus improve density specification for satellites flying in low Earth orbit (LEO).

14. SUBJECT TERMS	15. NUMBER OF PAGES
Vector Spherical Harmonic (VSH) Model	16. PRICE CODE

17. SECURITY CLASSIFICATION OF REPORT	18. SECURITY CLASSIFICATION OF THIS PAGE	19. SECURITY CLASSIFICATION OF ABSTRACT	20. LIMITATION OF ABSTRACT
Unclassified	Unclassified	Unclassified	Unlimited

Final Report: The VSH Model.

A. G. Burns and T. L. Killeen

The Vector Spherical Harmonic (VSH) model was originally developed to make the results of runs of the National Center for Atmospheric Research Thermospheric General Circulation Model (NCAR-TGCM) more accessible to scientific investigators. The original VSH model was a pure representation of the output fields of particular model runs, insofar as no interpolation was performed between model runs.

At the time investigators had problems accessing the output of the NCAR-TGCM for several reasons. The sheer size of the model meant that the only computers that it could run on at the time were supercomputers such as the Cray 1 at NCAR. This meant that a special request had to be registered at NCAR to make the model run. But even after the model was run, problems occurred because of the size of the output files. Depending on the length of the run, these could easily reach sizes of hundreds of megabytes, well beyond the capabilities of most transfer methods that were available in 1985. Even if they could have been transferred, there would have been considerable difficulties in storing and accessing these files on the local machines of most investigators.

The VSH model was first developed to solve these problems. By fitting Associated Legendre Polynomials to the output fields of the TGCM the data storage requirements were much reduced. This, in turn, meant that the output fields were much more accessible than hitherto.

The original VSH coefficients were limited to only three fields: the two components of the neutral wind and neutral temperatures. This last field was further limited by applying a Bates fit to the vertical. The disadvantage of this approach was that an important attribute of the GCM approach to thermospheric modeling was lost: the ability to consider cases where diffusive equilibrium was not appropriate.

Later it was realized that the VSH model was also capable of being a "stand-alone" model of the thermosphere, provided that suitable interpolations were made between model runs of the TGCM and its later incarnation the Thermosphere/Ionosphere General Circulation Model (the TIGCM). This model was developed, and the problem of the vertical representation was solved by replacing the Bates fit to the temperature with vertical splines. A minimal set of basis runs was developed and a version of this "hybrid" VSH model was distributed to the community.

This model provided a good representation of the quiet time thermosphere, but it was very limited in that the only representation of storm-time conditions involved an

extrapolation of the existing runs to times of high geomagnetic activity. Doing this had a number of weaknesses. The first one is that the auroral oval expands during geomagnetic storms, and the extrapolation of existing coefficients cannot represent this expansion. Second, the thermosphere does not immediately react to geomagnetic storms. There is a considerable delay in the density response, in particular, during which the thermospheric density increases "ramp up". Similarly, the thermosphere takes time to recover after the geomagnetic storm has ended. This report describes techniques that have been developed to provide a better thermospheric representation of these storm conditions. But first the NCAR-TIGCM and the basic implementation of the VSH model are described.

2. The NCAR-TIGCM

The NCAR-TIGCM (Thermosphere/Ionosphere General Circulation Model) is a three-dimensional, time-dependent model of the Earth's neutral upper atmosphere that is run on the CRAY-YMP computer at NCAR. The model uses a finite-differencing technique to obtain time-dependent solutions for the coupled, nonlinear equations of hydrodynamics, thermodynamics, and continuity of the neutral gas (*Dickinson et al.*, 1981; *Roble et al.*, 1982) and for the coupling between the dynamics and the composition (*Dickinson et al.*, 1984). A TIGCM, with a coupled ionosphere and a self-consistent aeronomic scheme, was developed by *Roble et al.* (1988). More recently, the model has been improved by including a self-consistent dynamo model (*Richmond et al.*, 1992). The latest developments in this suite of models include coupling with the stratosphere and mesosphere (*Roble and Ridley*, 1994). Detailed descriptions of the NCAR models, as well as their input parameterizations, have been given in papers by *Dickinson et al.* (1981, 1984), *Roble et al.* (1982, 1987, 1988), *Richmond et al.* (1992), and *Roble and Ridley* (1994).

Various publications have discussed the use of both the NCAR-TIGCM that is described above and the University College London-thermospheric general circulation model (UCL-TGCM - *Fuller-Rowell and Rees*, 1980, 1983; *Fuller-Rowell et al.*, 1987). These models have generally proved successful at reproducing the changes that are seen in the neutral thermosphere (e.g., *Crowley et al.*, 1989; *Burns et al.*, 1992a; *Fuller-Rowell et al.*, 1994).

The NCAR-TGCM used a variety of empirical and semi-empirical prescriptions and parameterizations, which were discussed in detail by *Roble et al.* (1984) and *Roble and Ridley* (1987). A brief description of these parameterizations is given here. The solar heating and photodissociation terms, described by *Dickinson et al.* (1981, 1984), were calculated from the *Hinteregger* (1981) solar EUV fluxes and the *Torr et al.* (1980) UV fluxes. The *Chiu* (1975) empirical model of electron density was supplemented by the addition of auroral particles using the prescription of *Roble and Ridley* (1987). The auroral oval prescription was similar to the statistical patterns described by *Spiro et al.* (1982) and *Whalen* (1983) and also those given by *Feldstein and Galperin* (1985). The ion drift velocities were specified by the magnetospheric convection model of *Heelis et al.* (1982), which includes displaced geomagnetic poles (north geomagnetic pole: 78.3N, 291.0E; south geomagnetic pole: 74.5S, 127.0E).

Although early versions of the VSH model used runs of the NCAR-TGCM as its basis, there were severe limitations in the utility of using this model as the basis of a thermospheric density specifications. A large number of inputs to the model used empirical paramaterizations rather than first principles calculations, which limited the accuracy of the model to the accuracy of these parameterizations. In addition, model temperatures were specified as a perturbation about a global mean, rather than as a complete calculation. Because the auroral inputs were an "add-on" to this global mean, it was very difficult to specify high latitude density and temperature structures adequately. Minor species neutral composition was not included in the TGCM, and it has become clear that these gases play a critical role in determining both the thermal and density structure of the thermosphere. Similarly, the lack of an interactive ionosphere required a reliance on the parameterized *Chiu* (1975) model in the TGCM.

In 1988, *Roble et al.* (1988) developed a version of the TGCM, the TIGCM, that addressed these problems. This coupled thermosphere/ionosphere model is a self-consistent coupled Eulerian model of the thermosphere and ionosphere. It utilizes the aeronomic scheme developed by *Roble et al.* (1987) and *Roble and Ridley* (1987). In this model the equations describing both the ionosphere and thermosphere are solved on the 5 degree by 5 degree grid mentioned in the previous section. The *Heelis et al.* (1982) model is still used to describe high-latitude motion, while the ion drifts at middle- and low-latitudes are described by the *Richmond et al.* (1980) empirical model, as they were for the TGCM. Displaced geomagnetic and geographic poles are used with a dipole magnetic field. Solar heating is now solved self-consistently once the external source of EUV and UV radiation is prescribed. Semi-diurnal tides have been included as a bottom boundary condition. In addition, the minor species ($N(^2D)$, $N(^4S)$, NO, He and Ar) and ion (O^+, O_2^+, NO^+, N_2+ and N^+) chemistry is calculated and the ion and neutral chemistry contributions to the thermal equation are assessed. In addition, the high-latitude ion and electron thermodynamic equations are solved for ion and electron temperatures.

The primitive equations that describe the NCAR-TIGCM are included in the next section. In order to develop the density specification model the TIGCM had to be tested and validated as well as developed. Over the years since it was first developed a number of studies have been undertaken that have performed this testing and validation. *Crowley et al.* (1989) first compared this model with data measured during solar minimum conditions, but most of their comparisons were done with the earlier TGCM. *Burrage et al.* (1992) compared output from the TIGCM with Atmosphere Explorer data at low latitudes. *Burns et al.* (1992a) compared the high-latitude response of a time-dependent

run of the model with the equivalent period of Dynamics Explorer 2 data, finding reasonable agreement between the two (Figure 2). *Burns et al.* (1992b) looked at both the recovery period after a geomagnetic storm and at low latitudes, again finding reasonable agreement between the model and data. As part of the Lower Thermosphere Coupling Study (LTCS), *Fesen and Roble* (1991) compared data from this campaign with a model simulation of the same period. They found that there was fair general agreement between the model calculations and observations of tidal structures. The following three diagrams give the basic structure of the three versions of the model.

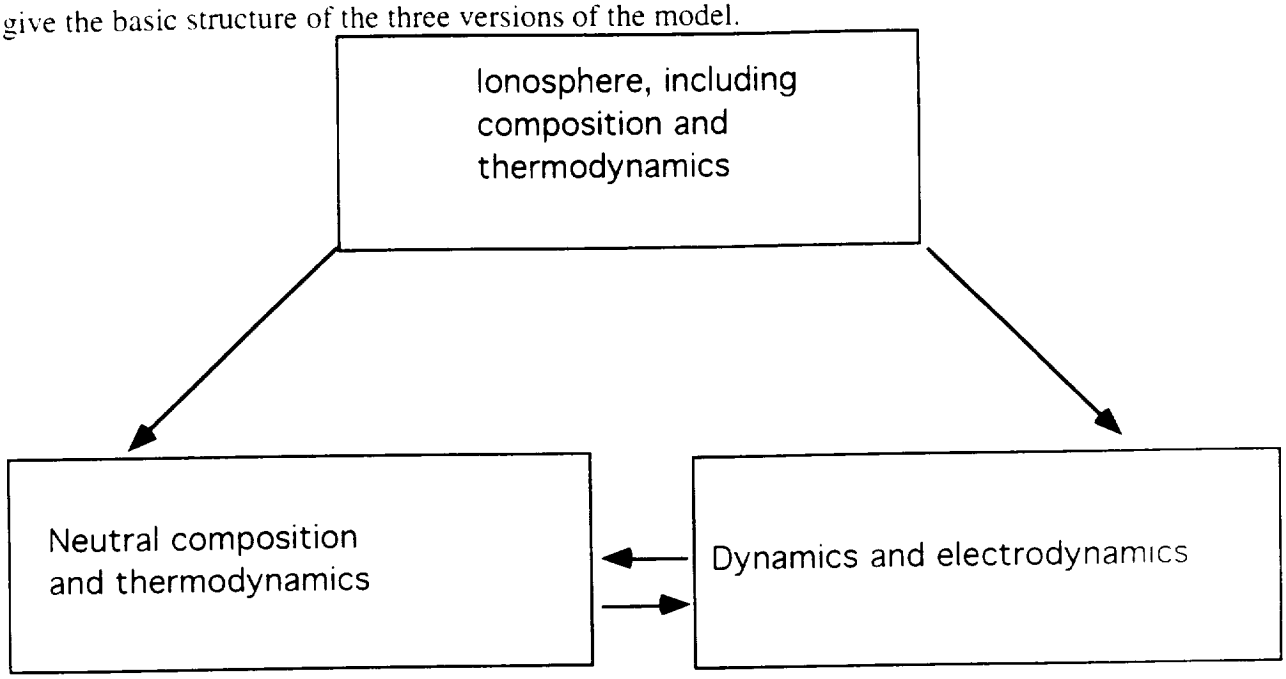

Figure 1 :TGCM

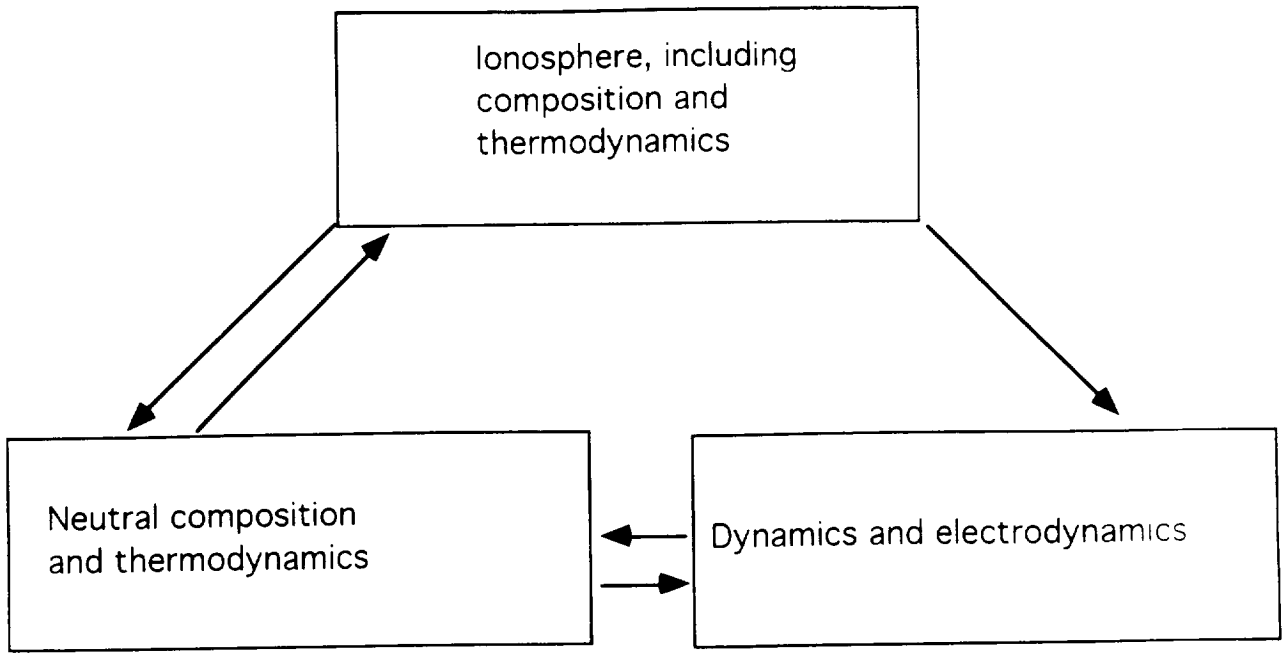

Figure 2: TIGCM

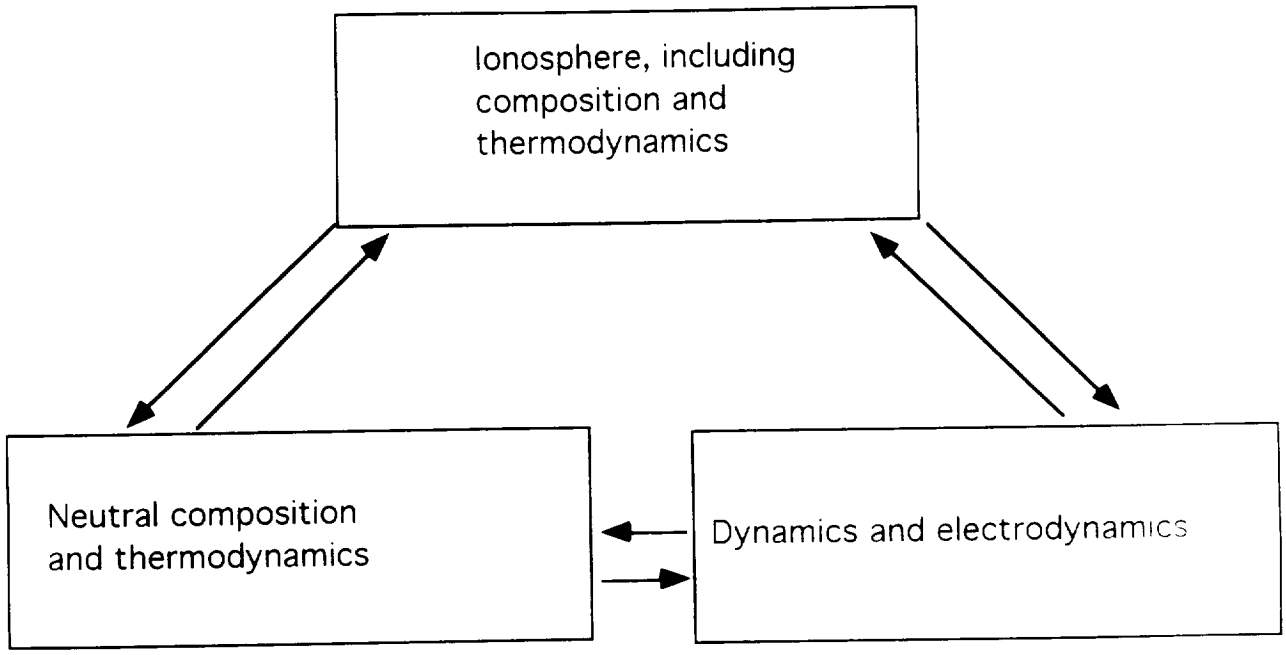

Figure 3: TIEGCM

Richmond et al. (1982) have described this new model, and the following discussion is based on their description. In addition to the self-consistent calculations of the dynamo

electric fields in the TIEGCM, another improvement over the earlier versions of the model has also been made. Earlier versions of the model used a dipole magnetic field model for the Earth's magnetic field. The new version of the model now uses a more realistic magnetic field model.

The ionospheric dynamo model uses the calculated neutral wind together with electric conductivities derived from the ion and neutral density distributions to compute the electric potential at each time step. Some of the essential features of the dynamo model are:

• Geomagnetic field lines are equipotentials, and current may flow between hemispheres along these lines at all magnetic latitudes outside of the polar caps (the boundaries of which can be varied, but are normally set to 75N and south)

• A realistic geomagnetic field (the International Geomagnetic Reference Field 1985) is used, with calculations being carried out in magnetic apex co-ordinates.

• The electric potential distribution is externally imposed within each polar cap, and is constrained within the auroral regions (set to be between 60 and 75 magnetic latitude in each hemisphere) to approach the *Heelis et al.* (1982) model near the polar cap boundary.

• The equatorial electrojet region is externally imposed.

All of these changes have the potential to create a more realistic ionosphere, which may, in turn, also produce a more realistic thermosphere.

Very large changes in the neutral wind occur in the equatorial region between the two versions of the model. In the fully coupled simulation, the upper nightside jet reaches wind strengths of 80 m/s as opposed to strengths of 30 m/s in the case where no atmospheric dynamo was included. Similarly, in the daytime the upper westward jet increased in speed from 30 m/s to 60 m/s. Lower in the thermosphere, the maximum wind speed in the nighttime eastward jet increases from 110 m/s to 140 m/s. In general, there are marked changes between the neutral thermospheric structure when the dynamo is and is not included.

3. The Equations Used in the NCAR-TIGCM

The NCAR-TIGCM solves the basic fluid equations in the upper atmosphere. These equations include: the continuity equation; the momentum equations: the thermodynamic energy equation: the minor species continuity equation: the O^+ transport equation: and the electron and ion energy equations. All of these equations are described here briefly.

The continuity equation for a single thermospheric species may be written in terms of the partial derivative with time of the mass mixing ratio, Ψ_i, of the i^{th} species. We use horizontal spherical coordinates and a log pressure vertical coordinate (λ, ϕ, z), where λ = longitude, ϕ = latitude and $z = \ln(P_0/P)$, P is the pressure, and P_0 (= 50 μPa) is a reference pressure, to write the following vector equation for the mass mixing ratio of each species (*Dickinson et al.*, 1984).

$$\frac{\partial}{\partial t}\tilde{\Psi} = -\frac{e^z}{\tau}\frac{\partial}{\partial z}\left[\frac{\bar{m}}{m_{N_2}}\left(\frac{T_{00}}{T}\right)^{0.25}\tilde{\alpha}^{-1}\mathbf{L}\tilde{\Psi}\right] + e^z\frac{\partial}{\partial z}\left[K(z)\,e^{-z}\frac{\partial}{\partial z}\left(1+\frac{1}{\bar{m}}\frac{\partial\bar{m}}{\partial z}\right)\tilde{\Psi}\right] - \left[\vec{V}.\nabla\tilde{\Psi} + w\frac{\partial}{\partial z}\tilde{\Psi}\right] + \tilde{S} - \tilde{R} \qquad (1)$$

The terms on the rights hand side of this equation represent, respectively, the changes in the composition due to molecular diffusion, eddy diffusion, horizontal and vertical advection, and chemical production and loss. The $\left(1+\frac{1}{\bar{m}}\frac{\partial\bar{m}}{\partial z}\right)$ term is included in the eddy diffusion calculations to account for variations in the mean molecular mass with height which affect the eddy diffusion rate. The vector mass mixing ratio is given by Ψ = (Ψ_{O2} ,Ψ_O) and Ψ_i is defined by:

$$\Psi_i = \frac{n_i m_i}{\sum n_j m_j} \qquad (2)$$

$\vec{V}$ = the horizontal velocity vector; u = the eastward neutral velocity; v = the northward neutral velocity; w = the vertical neutral velocity; T = temperature; n_i = number density of the i^{th} species, and m_i is the mass of the i^{th} species. Other parameters include D, the molecular diffusion coefficient given by

$$D = D_0 \left[\frac{P_{00}}{P}\right]\left[\frac{T}{T_{00}}\right]^{1.75} \tag{3}$$

where D_O is a characteristic diffusion coefficient at pressure P_{OO} and temperature T_{oo} (= 2×10^{-1} cm2 s-1), H_o is the characteristic molecular nitrogen scale height at T_{oo} = 273K (= 8.63km), J_{O2} is the molecular oxygen photodissociation rate; k is a rate coefficient for three-body ($O + O + M \rightarrow O_2 + M$) recombination of atomic oxygen given by $k = 3.8 \times 10^{-30} \exp(-170/T)/T$ for $M = O_2$ (*Johnston*, 1968) and $k = 4.8 \times 10^{-33}$ for $M = N_2$ (*Campbell and Gray*, 1973). K(z) is the eddy diffusion coefficient, $\overline{m}$ the mean mass, P_{oo} is the atmospheric pressure at the ground (= 10^5 Pa), T_{OO} = 273K, δ_{ij} is the delta function, τ is the diffusion time scale. The mixing ratio of N_2 is defined as

$$\Psi_{N_2} = 1 - \Psi_{O_2} - \Psi_O \tag{4}$$

Photodissociation provides a source of O given by:

$$\bar{S} = J_{O_2}\begin{bmatrix} -\Psi_{O_2} \\ \Psi_{O_2} \end{bmatrix} \tag{5}$$

and three body recombination provides a source of O_2. The alpha coefficients in the first term on the right hand side of equation 1 are given by:

$$\begin{aligned}
\alpha_{11} &= -\left[\phi_{13} + \left(\phi_{12} - \phi_{13}\right)\Psi_2\right] \\
\alpha_{22} &= -\left[\phi_{23} + \left(\phi_{21} - \phi_{23}\right)\Psi_1\right] \\
\alpha_{12} &= \left(\phi_{12} - \phi_{13}\right)\Psi_1 \\
\alpha_{13} &= \left(\phi_{21} - \phi_{23}\right)\Psi_2
\end{aligned} \tag{6}$$

where the subscript $_1$ denotes O_2; $_2$ denotes O; and $_3$ denotes N_2 and the ϕ_{ij} are defined by:

$$\phi_{ij} = \left(\frac{D}{D_{ij}}\right)\left(\frac{m_3}{m_j}\right) \tag{7}$$

where D_{ij} is the mutual diffusion coefficients given by *Colegrove* (1966). The matrix operator **L** has elements:

$$L_{ij} = \delta_{ij}\left(\frac{\partial}{\partial z} - \varepsilon_{ij}\right) \tag{8}$$

where ε_{ii} is defined by

$$\varepsilon_{ii} = 1 - \frac{m_i}{\bar{m}} - \frac{1}{\bar{m}}\frac{\partial \bar{m}}{\partial z} \tag{9}$$

The L matrix defines diffusive equilibrium solutions through the equation $\mathbf{L}\,\bar{\Psi}=0$. Departures from diffusive equilibrium are driven by the hydrodynamic transport and the chemical terms in equation 1.

The next equations of interest are the eastward momentum equation

$$\frac{\partial u}{\partial t} = \frac{g e^z}{P_0}\frac{\partial}{\partial z}\left(\frac{\mu}{H}\frac{\partial u}{\partial z}\right) + f\,v + \left\{\lambda_{xx}(u_i - u) + \lambda_{xy}(v_i - v)\right\}$$

$$+ \left\{-\mathbf{V}.\nabla u + \frac{u\,v}{r}\tan\phi\right\} - \frac{1}{r\cos\Phi}\frac{\partial \Phi'}{\partial \lambda} - w\frac{\partial u}{\partial z} \tag{10}$$

and the northward momentum equation

$$\frac{\partial v}{\partial t} = \frac{g\,e^z}{P_0}\left(\frac{\mu}{H}\frac{\partial v}{\partial z}\right) - f\,u + \left\{\lambda_{yy}(v_i - v) + \lambda_{yx}(u_i - u)\right\}$$

$$+ \left\{-\mathbf{V}.\nabla v - \frac{u^2}{r}\tan\phi\right\} - \frac{1}{r}\frac{\partial \Phi'}{\partial \phi} - w\frac{\partial v}{\partial z} \tag{11}$$

The thermodynamic energy equation is no longer expressed in terms of perturbations

$$\frac{\partial T}{\partial t} = \frac{g\, e^{z}}{P_0\, C_p} \frac{\partial}{\partial z} \left\{ \frac{K_T}{H} \frac{\partial T}{\partial z} + K_E H^2 C_p \rho \left(\frac{g}{C_p} + \frac{1}{H} \frac{\partial T}{\partial z} \right) \right\}$$

$$- \mathbf{V}.\nabla T - w \left(\frac{\partial T}{\partial z} + \frac{R\, T}{C_p\, \bar{m}} \right) + \frac{Q_{ph}}{C_p} + \frac{Q_{ic}}{C_p} + \frac{Q_{mc}}{C_p} + \frac{Q_J}{C_p}$$

$$+ \frac{Q_s}{C_p} - \frac{L_{rad}}{C_p} \qquad (12)$$

The minor species compositional equation describes the odd nitrogen species (NO, $N(^4S)$ and $N(^2D)$

$$\frac{\partial \Psi_n}{\partial t} = - e^{z} \frac{\partial}{\partial z} \left\{ A_n \left(\frac{\partial}{\partial z} - E_n \right) \Psi_n \right\} + S_n - R_n$$

$$- \left(\mathbf{V}.\nabla \Psi_n + w \frac{\partial \Psi_n}{\partial z} \right)$$

$$+ e^{z} \frac{\partial}{\partial z} \left\{ e^{-z} K_E(z) \left(\frac{\partial}{\partial z} + \frac{1}{\bar{m}} \frac{\partial \bar{m}}{\partial z} \right) \Psi_n \right\} \qquad (13)$$

The ionosphere is described by the following equations. The O^+ transport equation.

$$\frac{\partial n_{O^+}}{\partial t} = P_{O^+} - L_{O^+} - \nabla.n_{O^+}\mathbf{V}_i \qquad (14)$$

Where the ion velocity has parallel and perpendicular components

$$\mathbf{V_i} = \mathbf{V_{//}} + \mathbf{V_\perp} \qquad (15)$$

$$\mathbf{V_{//}} = \left\{ \mathbf{b}.\frac{1}{\upsilon}\left[g - \frac{1}{\rho_i}\nabla (P_i + P_e) \right] + \mathbf{b}.\mathbf{V} \right\} \mathbf{b}$$

$$\mathbf{V_\perp} = \frac{1}{|\mathbf{B}|}\mathbf{E} \times \mathbf{b}$$

The time rate of change of ion and electron temperature is assumed to be small compared with the time scale of the TIGCM, so a quasi-thermal equilibrium can be assumed for these temperatures. That is, the rate at which the ion and electron temperatures change as a result of other heating processes is sufficiently fast that we can ignore heat transport.

The electron energy equation is given by

$$\sin^2 I \frac{\partial}{\partial z}\left(K_e \frac{\partial T_e}{\partial z} \right) + Q_e - L_e = 0 \qquad (16)$$

$L_e = L_{ei}$ (coulomb collisions with ions)

$+ L_{en}$ (elastic and inelastic collisions with neutrals)

The cooling rates that occur as a result of coulomb collisions with ions are given by

$$L_{ei} = 3.2 \times 10^{-8} n_e \frac{(T_e - T_i)}{T_e^{3/2}} \ln \Lambda \times$$

$$\{ n(O^+) + 0.5\, n(O_2^+) + 0.53\, n(NO^+) \} 1.602 \times 10^{-12}$$

The electron cooling rates that result from elastic and inelastic collisions with neutrals are given by

$$L_{en} = \{ L(e, N_2) + L(e, O) + L(e, O_2) + L(e, N_2)_{vib}$$

$$+ L(e, O_2)_{vib} + L(e, O)_{fine} + L(e, O)_{excit\ ^1D}$$

$$+ L(e, N_2)_{rot} + L(e, O_2)_{rot} \} 1.602 \times 10^{-12}$$

The ion energy equation.

$$T_i = T_n \left(\frac{\upsilon_{in}}{\upsilon_{in} + \upsilon_{ie}} \right) + T_e \left(\frac{2\, \upsilon_{ie}}{\upsilon_{in} + \upsilon_{ie}} \right) + \frac{\upsilon_{in}\, m_O}{3k (\upsilon_{in} + \upsilon_{ie})} (\mathbf{v}_i - \mathbf{v})^2 \qquad (17)$$

These equations provide the basis for the calculation of the thermosphere ionosphere system. Numerical methods are used to solve them simultaneously, and the resulting output fields provide the basis for the VSH model. Before describing the numerical schemes used in the VSH model, it is necessary to discuss some problems which eventually prevented us from using the electrodynamics version of the TGCM.

4. Problems with using the NCAR-TIEGCM

It was originally intended to develop the VSH model further using output files generated by the NCAR-TIEGCM. Unfortunately, model validation of this version of the model did not proceed as rapidly as was anticipated at the time of the original proposal.

In the first year and a half of the current contract coefficient, files were developed to replace the original TIGCM files. All of the requisite quiet-time model runs, except three were made. The last two were indicative of one of the problems that still occurred in the TIGCM. These three runs were made during solar maximum conditions, and were for geomagnetically active times, with cross cap potentials of 90. In these conditions the model blew up relatively soon after the beginning of the day. In the past this has indicated problems with shear in the convection pattern. The problem gets worse as attempts are made to run the model for storm conditions.

The other problem that was found during this time is more fundamental, and has since been solved, but it indicates that far more intensive testing of the NCAR-TIEGCM needs to be undertaken before it is used for anything other than a pure research tool. It was found that the electron densities at high latitudes in the TIEGCM (but not in the TIGCM) were far higher than could be reasonably expected. This has ramifications not only for ionospheric specification, but also for the specification of the neutral thermosphere. If electron densities are two large at high latitudes, two things happen that affect the neutral thermosphere. First, ion-neutral coupling rates will increase rapidly altering the advective distribution of the neutral species and through the pressure gradient force the rate of vertical transport of constituents and global heating rates through adiabatic expansion and compression. The second consequence is that the distribution of Joule heating will change. Overall specification of the neutral thermosphere will be in error.

As was stated this particular problem has been solved, but it is indicative that to this time adequate testing of the NCAR-TIEGCM has yet to be carried out. Given these circumstances, it was felt that the TIEGCM was not yet ready to be used as an operational model that could provide input to the VSH model.

5. VSH Formulation

The VSH model acts on the output fields from the NCAR-TIGCM. These fields are fitted spectrally by a set of Associated Legendre polynomials, and sets of coefficient files are derived for a variety of different geophysical conditions. The output from the model is then obtained by synthesizing these different coefficient files to produce output results that are appropriate to the conditions that were put into the model.

The spectral fit consists of using smooth curves to represent the variation of any output variable (such as mass mixing ratio or temperature) with respect to any input variable (such as latitude or ap). Each input/output relation is defined by 1) identifying a familiar, easily computable, family of curves (the basis functions) and 2) determining the best fitting linear combination of the basis functions to represent the actual atmospheric variations. Familiar examples of basis functions include the cosine and sine functions in a Fourier fit, and the polynomial functions in a least-squares fit. The weights that make up the linear combination of the fit - the spectral coefficients - are what is actually stored in the coefficient libraries.

This process of fitting spectral coefficients on the Cray, then reconstituting them in VSH, has two important features associated with it. First, the series generating the spectral coefficients are truncated at levels that reduce the computer storage requirements but retain the important variations of the output fields. In this way, computers of modest storage capabilities can take advantage of the results of a general circulation model over a wide range of geophysical conditions.

The second feature of this process is that a model based on discrete grid points, discrete times, and discrete geophysical conditions is converted into a model that is continuous over these same variables. The nature of the interpolation over each of its continuous domains is described in the following sections. It should be pointed out that some of the interpolations (such as the variation over solar activity) are actually carried out across several TIGCM runs (rather than within a run).

Horizontal

On a sphere, the spherical harmonics are the most natural basis functions to describe the latitudinal and longitudinal variations of a scalar variable. The spherical harmonics are represented mathematically as:

$$Y_n^m(\theta,\lambda) = P_n^m(\cos\theta)\ e^{im\lambda} \qquad (18)$$

where the functions P are the Legendre polynomials, q is colatitude, and l is longitude. The value of a scalar quantity (e.g. mass density or temperature) at a particular location is calculated in VSH from the sum:

$$q(\theta,\lambda) = \sum_{m,n} a_{m,n}\ Y_n^m(\theta,\lambda) \qquad (19)$$

The coefficients $a_{m,n}$ are complex quantities because of the multiplication by e^{iml}. That is, the real part of $a_{m,n}$ will be multiplied by cos ml and the imaginary part will be multiplied by sin ml.

Despite the complicated mathematical form of the spherical harmonics, these functions are well understood and their values are easily calculated. The need for this level of sophistication arises because of the convergence of the longitudinal lines at the poles (where singularities can occur). The use of spherical harmonics allow the output fields to retain continuity across the poles.

For vector variables, a further consideration is required. The coordinate system is singular at the poles, because north and south wind directions are not continuous at the poles. A change of coordinates is carried out by expressing the wind as the sum of a gradient with zero curl (the velocity potential x) and a curl with zero gradient (the streamfunction y). That is, the horizontal wind field can be given as

$$\vec{U}(\theta,\lambda) = \nabla\xi(\theta,\lambda) + \nabla \times \vec{k}\,\psi(\theta,\lambda) \qquad (20)$$

In spherical coordinates, this vector equation is equivalent to the set

$$u(\theta,\lambda) = \frac{1}{r\sin\theta}\frac{\partial\xi}{\partial\lambda} + \frac{1}{r}\frac{\partial\psi}{\partial\theta}$$
$$v(\theta,\lambda) = -\frac{1}{r}\frac{\partial\xi}{\partial\theta} + \frac{1}{r\sin\theta}\frac{\partial\psi}{\partial\lambda} \qquad (21)$$

where r is the radius of the earth.

The velocity potential x and the streamfunction y are scalar variables that can be represented as sums of spherical harmonics using (19) and (20):

$$\xi(\theta,\lambda) = r \sum_{m,n} b_{m,n} Y_n^m(\theta,\lambda)$$
$$\psi(\theta,\lambda) = r \sum_{m,n} c_{m,n} Y_n^m(\theta,\lambda) \qquad (22)$$

(The radius of the earth r is introduced as a normalization factor.) Using the identities

$$\frac{\partial Y}{\partial \theta} = \frac{\partial P}{\partial \theta} e^{im\lambda} \qquad \frac{\partial Y}{\partial \lambda} = im\, P\, e^{im\lambda} \qquad (23)$$

and inserting (23) and (24) into (22): yields the formula for recreating winds from vector spherical harmonic coefficients $b_{m,n}$, $c_{m,n}$:

$$\begin{bmatrix} u \\ v \end{bmatrix} = \sum_{m,n} \left\{ b_{m,n} \begin{bmatrix} \frac{im\,P}{\sin\theta} \\ \frac{-\partial P}{\partial \theta} \end{bmatrix} + c_{m,n} \begin{bmatrix} \frac{\partial P}{\partial \theta} \\ \frac{im\,P}{\sin\theta} \end{bmatrix} \right\} e^{im\lambda} \qquad (24)$$

The distinction between scalar variables (such as temperature or density) and vector variables (such as neutral wind) is summarized in the table below.

Variable	Basis
Scalars	$P_n^n e^{im\lambda}$
Vectors	$\frac{m\,P}{\sin\theta} e^{im\lambda}$, $\frac{\partial P}{\partial \theta} e^{im\lambda}$

That is, scalars use a scalar basis function, while vectors use a vector basis. The functions

$$P_n^m \quad , \quad \frac{m\,P_n^m}{\sin\theta} \quad , \text{ and } \quad \frac{\partial P_n^m}{\partial \theta}$$

are precomputed.

The coefficient values, b and c, that go into the libraries were computed by performing a least-squares fit to minimize the squared error in the spectral representation. The algorithm for performing the least-squares fit is described in *Schwarztrauber* (1981). The actual values of the streamfunction and velocity potential are normalized by a division by $\sqrt{n(n+1)}$ where n is the meridional index.

Vertical

The vertical structure of a geophysical field is described by the least squares fit of a spline (a piecewise polynomial). A spline of degree n is defined as a piecewise polynomial of degree n, for which each of the first n-1 derivatives is continuous. Therefore, a cubic spline is a function that is continuous and for which its first two derivatives are continuous. The coefficients that define the cubic will generally vary from one subinterval to another.

The motivation for the use of splines to represent vertical variations, is that different physical processes occur at different altitudes. As a result, the vertical profiles vary greatly with altitude.

In the TIGCM, the vertical variable is log pressure rather than geometric height. Therefore, the vertical representation of each of the dependent variables is carried out as a function of log pressure. Geometric height is also a dependent variable (as a function of log pressure) with its own set of coefficients in the coefficient library. Therefore, when a VSH user inputs an altitude, the spline defining altitude versus log pressure is inverted to convert the altitude to a log pressure. This log pressure can then be used to retrieve any of the desired output fields. The inversion of the altitude spline is carried out via a Newton-Raphson method of finding real roots.

In the VSH model, cubic splines are used in the altitude range of 110-500 km at solar maximum. Above about 500 km at solar maximum, the MSIS model is called. The 110-500 km range is divided into several subintervals, in each of which the polynomial has different coefficients. Each end point of the subinterval is known as a knot. The altitude range is different during solar minimum conditions due to the different heights of the pressure surfaces, but the principles behind the vertical fit are much the same.

Temporal

For both the storm and quiet cases, the spherical harmonic fit described above is performed at every hour of model time. A temporal fit then needs to be made. No spectral representation is possible in the storm case so all times have to be used. But the quiet-time TIGCM runs produce diurnally reproducible results. A temporal representation can be used to capture the variations of the spherical harmonic coefficients over the course of a day. A Fourier time series is used for this purpose.

A Fourier representation implicitly assumes that the output fields are periodic: that is, it is assumed that the fields reproduce themselves on a daily basis. This assumption is not valid during times of transient magnetic storm activity. The storm subset of VSH does not perform a spectral fit over the course of a magnetic storm, but instead records information for each hour of storm time.

The Fourier fit for the daily variation of any field is represented as follows:

$$a_{m,n,z} = \frac{a_{0,m,n,z}}{2} + \sum_{k=1}^{T} a_{k,m,n,z} \cos kt + \sum_{k=1}^{T} b_{k,m,n,z} \sin kt \qquad (25)$$

Seven coefficients are retained (T=3). This represents a constant term plus three (time) symmetric coefficients plus three (time) antisymmetric coefficients (diurnal, semidiurnal, and terdiurnal).

6. Formulation of a "Storm" VSH model.

In the original VSH formulation, a set of coefficients was developed for quiet geomagnetic times. Later it was realized that such a set of coefficients was inaccurate at just those times when thermospheric models were most needed to provide specifications for various fields: during geomagnetic storms. Therefore it was decided to develop a time-dependent version of the VSH model to create a complete VSH model that was applicable to a wide variety of geophysical conditions.

Instead of using just one value of Ap, the time-dependent VSH model uses a 24 hour time history of three-hourly ap values, running from a time 24 hours prior to the time of observation up to the time of observation. Many problems occur in developing a model to simulate conditions during geomagnetic storms, not least of which is the problem of the time of storm onset. This introduces another degree of freedom into the problem. In the old version of the VSH model, time is represented as a set of Fourier coefficients that describe a diurnally reproducible run. Now, with the storm version of the model, this quiet time UT dependence of the location of the geomagnetic pole not only has to be taken into account, but the time after the storm start also has to be considered. One possible solution to this problem would be to make a storm-time run for each one or two hours of storm time and use this to drive the model. However, doing this increases the storage requirements of the model considerably and still does not deal with some outstanding problems, such as the duration of the storm, and the need to normalize the TIGCM to produce accurate densities in this case. Rather than this approach, we used the results of research done by Prölss and others (e. g., *Prölss*, 1980) which showed that the response of the neutral thermosphere to geomagnetic storms is much better oriented in geomagnetic rather than geographic space. Using this concept, we were able to develop a version of the model that used storm-time perturbation additions to baseline, diurnally-reproducible cases.

Before going into the mechanics of the storm-time version of the model further, it is worth examining why such a model is necessary, and why the previous technique of extrapolating from time-dependent, diurnally-reproducible runs that were developed for active conditions were not entirely successful.

One major feature of geomagnetic storms is that, unlike the magnetosphere and the ionospheric convection pattern, the neutral thermosphere takes some time to respond to the onset of geomagnetic storms. The time delay for these changes can vary between

about half an hour and several hours, depending on the prevailing geophysical conditions (*Ponthieu et al.*, 1988). Extrapolation techniques do not allow us to incorporate such a delay into the model.

Another feature that occurs during geomagnetic storms is the large transients that are set up early in the storm (e.g., *Mayr et al.*, 1984; *Burns and Killeen*, 1992a). These transients are produced during storm-time runs of the TIGCM, but, naturally, do not occur in diurnally reproducible runs. Again, this requires a fully time-dependent model.

The effects of geomagnetic storms on the neutral thermosphere do not terminate abruptly. Instead, there is a long "tail-off" as various processes (especially the effects of NO cooling- *Maeda et al.*, 1989; *Burns et al.*, 1989) act both directly and indirectly to restore the neutral thermosphere to its quiet-time state. A time-dependent model is needed to reproduce this "tail-off".

As well as these physical reasons for improving the ability to model the time-dependent response of the thermosphere to geomagnetic storms, there is a programmatic one as well. The present models used to simulate thermospheric densities do a particularly poor job during geomagnetic storms. Evidence comes for this in the number of satellites lost during geomagnetic storms and the breakdown in communications at this time. The latter may be thought to be an ionospheric problem, but, since *Matsushita*'s work in 1959, evidence has accumulated that the loss of electrons in the high-latitude F region at this time is largely due changes in neutral composition. Thus, if you want to develop an adequate model of the ionosphere, you must use a suitable model of the neutral thermosphere that includes all of the composition, circulation and thermal changes that occur during geomagnetic storms. The time-dependent VSH model does this.

One of the problems that occurs in attempting to model geomagnetic storms is that the thermospheric response to them is still one of the most active areas of thermospheric research. In attempting to develop a parametrical model of the thermosphere at these times a number of questions had to be posed that have still not been researched properly. One such question is the way that the thermosphere changes in response to high-latitude forcing and the length of time that this takes. Similarly, the way that the thermosphere recovers after the ion forcing and the length of time that this takes is also not well understood. Figure 4 and Figure 5 show our first attempts to study this situation. In our first attempt to solve some of these problems we assumed that thermospheric temperatures, and by implication densities, would be "saturated" in 6 hours (Figure 4). This Figure was produced by averaging all temperature values at latitudes greater than 60 N for winter conditions at solar minimum. Similar studies were done in the summer

hemisphere and for solar maximum conditions. In this case, the maximum value of ap was 50 and the storm ran for six hours after the onset. The horizontal axis refers to the time after the onset of the storm in hours (storm commencement was 10 UT). The vertical axis is the percentage increase in temperature between the storm run and the equivalent quiet-time diurnally reproducible case.

As can be seen from this graph, temperatures kept increasing for an hour or two after the storm had ceased. It is plain that temperatures did not "saturate" during a storm of 6 hours duration. Therefore, we increased the duration of the storm to 12 hours (Figure 5).

Now, maximum average temperatures occur some 10 hours after the storm commencement, still two hours before ionospheric forcing ended. It is likely that "saturation" has occurred and, thus, that this storm duration could be used as the basis for our time-dependent model.

The recovery time after the storm presents even greater problems. Little work has been done to categorize this recovery. *Hedin et al.* (1977) looked at a set of data from the AE satellites to categorize many features of geomagnetic storms. They also looked at storm-time recovery in a limited way. Their study and a subsequent one by *Porter et al.* (1981), made using the same data, produced a simple empirical relationship that was used to formulate the recovery period in the MSIS model. It is likely that the parameterizations used were to simple to model recovery adequately, although this hypothesis has not been rigorously tested using independent experimental data.

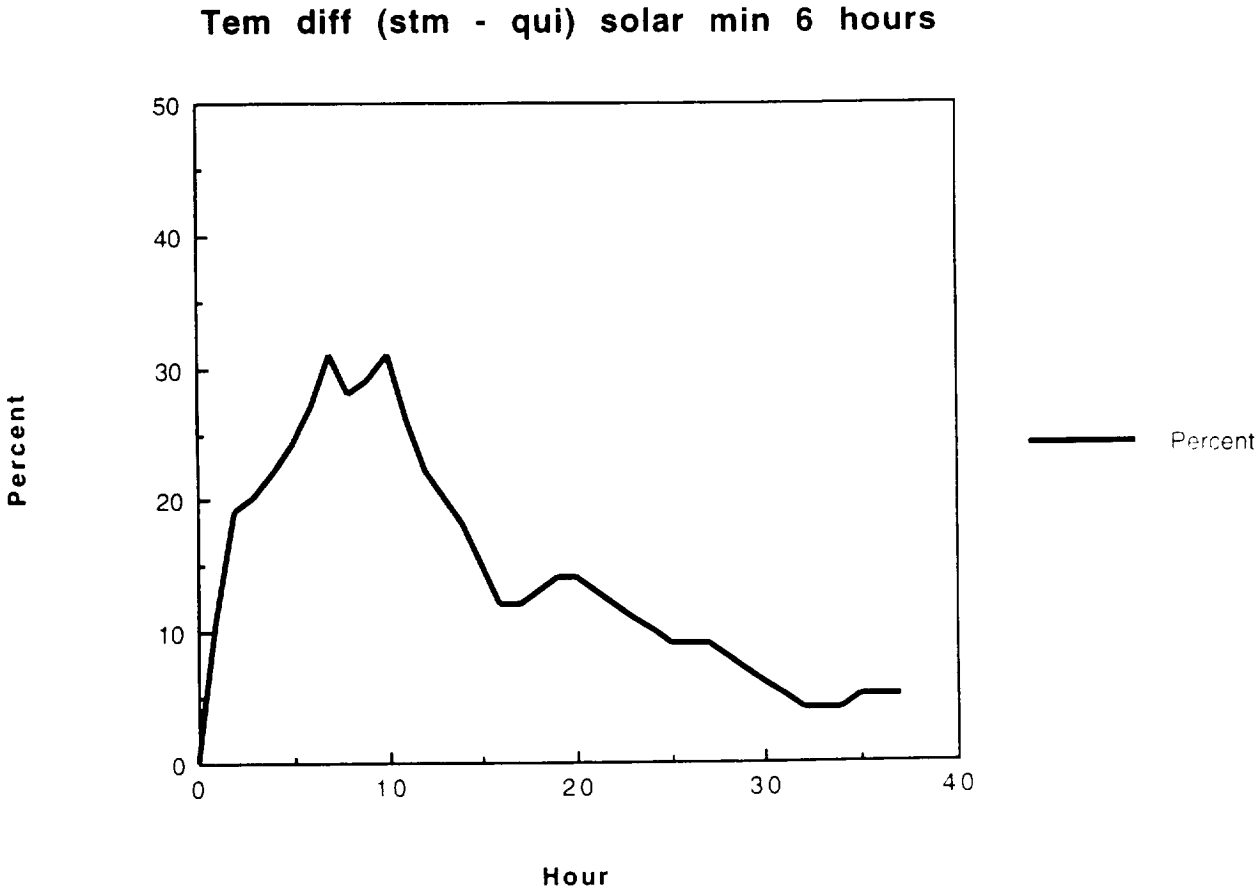

Figure 4. Temperature changes north of 60 degrees for a storm of 6 hours duration.

This problem was not addressed again with the use of experimental data for another decade. *Burns and Killeen* (1992 b) used results from an unpublished manuscript as part of a review of the thermospheric composition changes that occur during geomagnetic storms. They found a relatively "clean" storm, where there were good data from the recovery period. By "clean" we mean that the storm was of relatively short duration and that the period preceding the storm was quiet for a considerable time. Thus, contamination from previous storms was unlikely to be a problem. Furthermore, the "cut-off" or cessation of magnetospheric forcing at the end of the storm was very sharp, a result of a strong northward turning in the z component of the interplanetary magnetic field at this time.

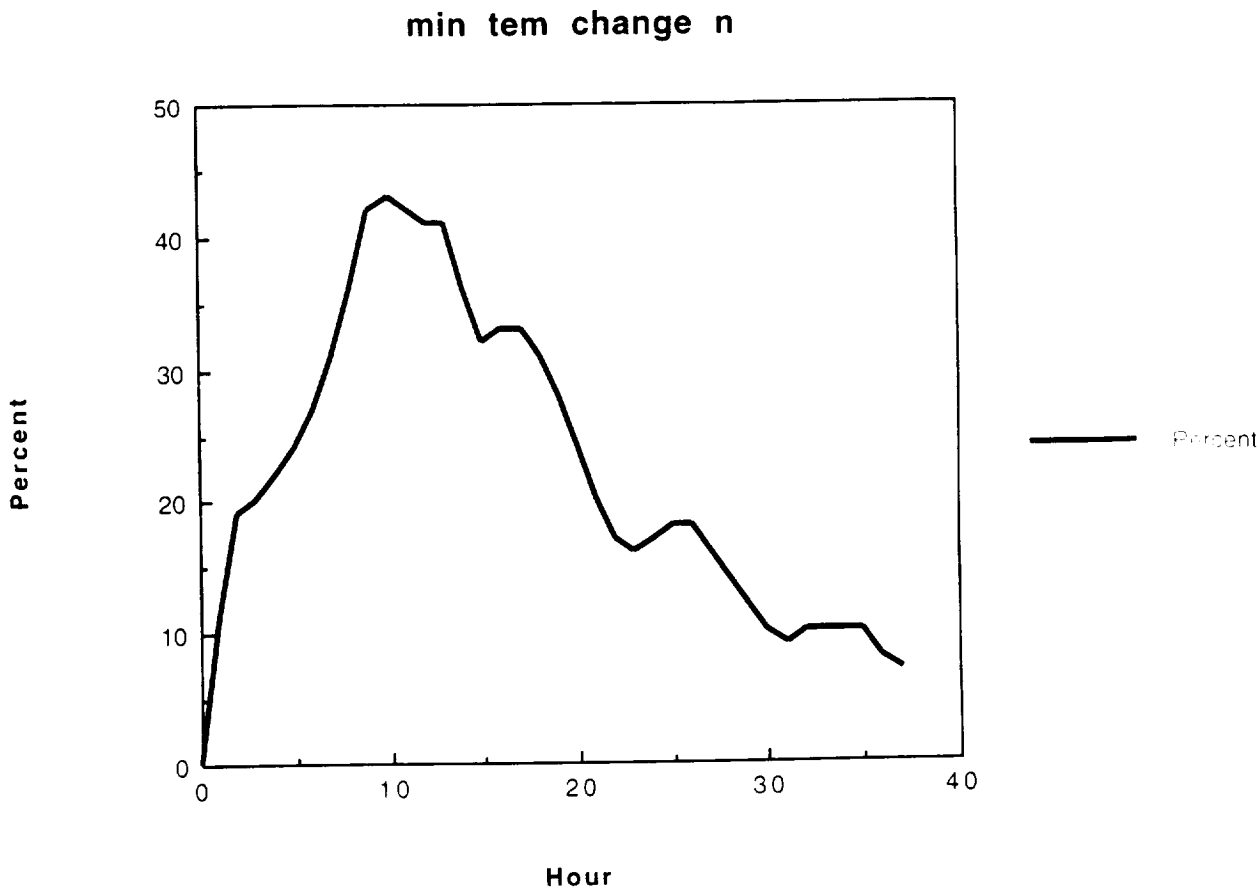

Figure 5. Temperature changes north of 60 degrees for a storm of 12 hours duration.

Perhaps of greatest interest of this study to the development of a hybrid model of the thermosphere is the duration of the recovery period. It is clear that, within 18 hours of the end of the storm, no decrease in the ratio is present and that 50% of the recovery has occurred within 6 or 7 hours after the end of the storm. Temperature recovery is even faster, suggesting that density recovery will be rapid after the end of the storm. Another interesting feature of the recovery is that it is not uniform. It occurs first at the poles, and then progressively at lower latitudes.

The TIGCM reproduces the major features of this plot. The recovery time within the model is similar and the tendency to recover first at high latitudes is also modeled successfully. Thus, we can be reasonably confident that the time of recovery indicated in Figure 5 is similar to that which occurs in the real thermosphere, and that the gross

features of this recovery are well represented. Thus, we were able to use the TIGCM recovery scheme in our time-dependent VSH model with little modification.

Considerations such as those mentioned above determined the structures that we would use to develop the time-dependent VSH model. The precalculation of the difference fields that was necessary to produce this model made it easier to apply interpolation schemes to the storm effects without modifying the underlying base model that was dependent on the other geophysical conditions.

The basic model structure is that difference coefficient fields are calculated in geomagnetic coordinates. These difference fields are then used as "add-ons" to existing coefficient files that supply the underlying, non geomagnetically forced, background thermosphere. There was a minimum requirement of an additional 12 TIGCM runs to produce these difference fields, but their modular arrangement makes it easy to omit them if time is a more important concern than accuracy.

The technique of producing these files is outlined in Figure 6.

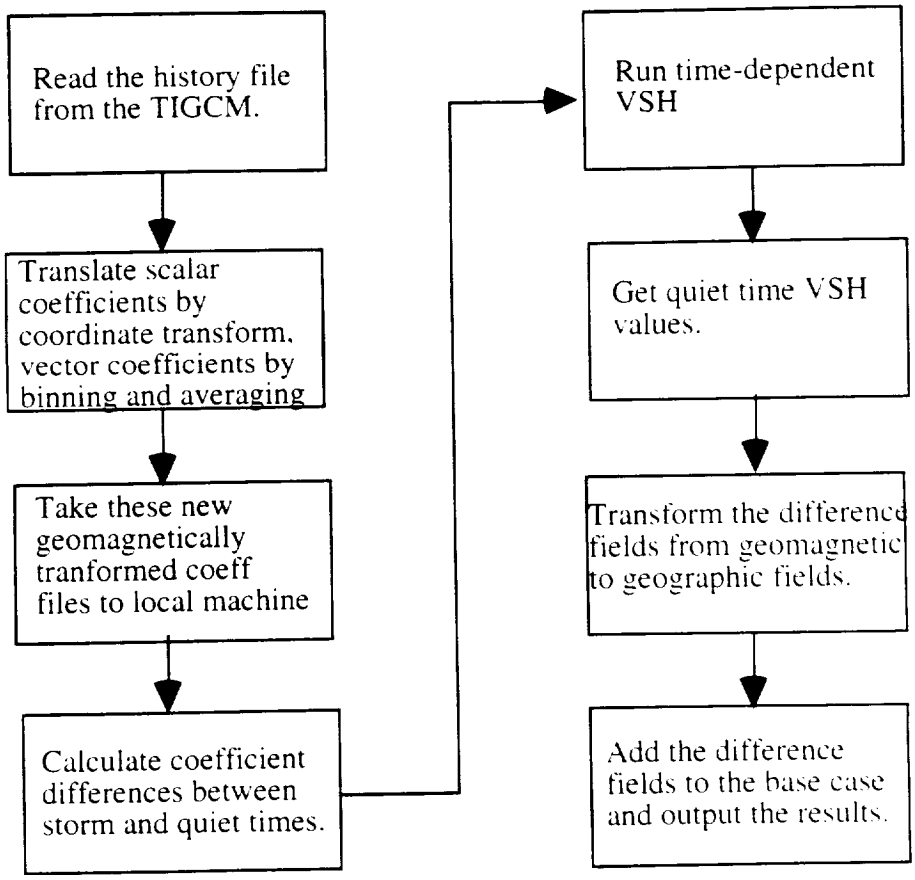

Figure 6: The time-dependent VSH Technique.

A problem that arose in developing the time-dependent model was how best to represent the changes that occur with time. Previously, the VSH model had always used a Fourier transform to reduce the number of coefficients needed. The initial version of the time-dependent VSH model also used this scheme. However, it was soon found that this resulted in spurious information being included in the model output, so it was decided to produce one coefficient set for each hour of storm-time.

7. Comparisons Between the VSH Models and SETA Data (solar maximum conditions).

The storm VSH model was first compared with SETA (Satellite Electrostatic Triaxial Accelerometer) data for a set of 14 randomly selected days from June 1982. On two of the days there was almost continuous storm conditions prevailing, while on another day there was a long period during which a storm occurred, and a recovery period.

The results of this study are shown in Figure 7. In this Figure the time-dependent VSH model standard deviations are compared with those calculated by MSIS and with those calculated by the non time-dependent VSH model.

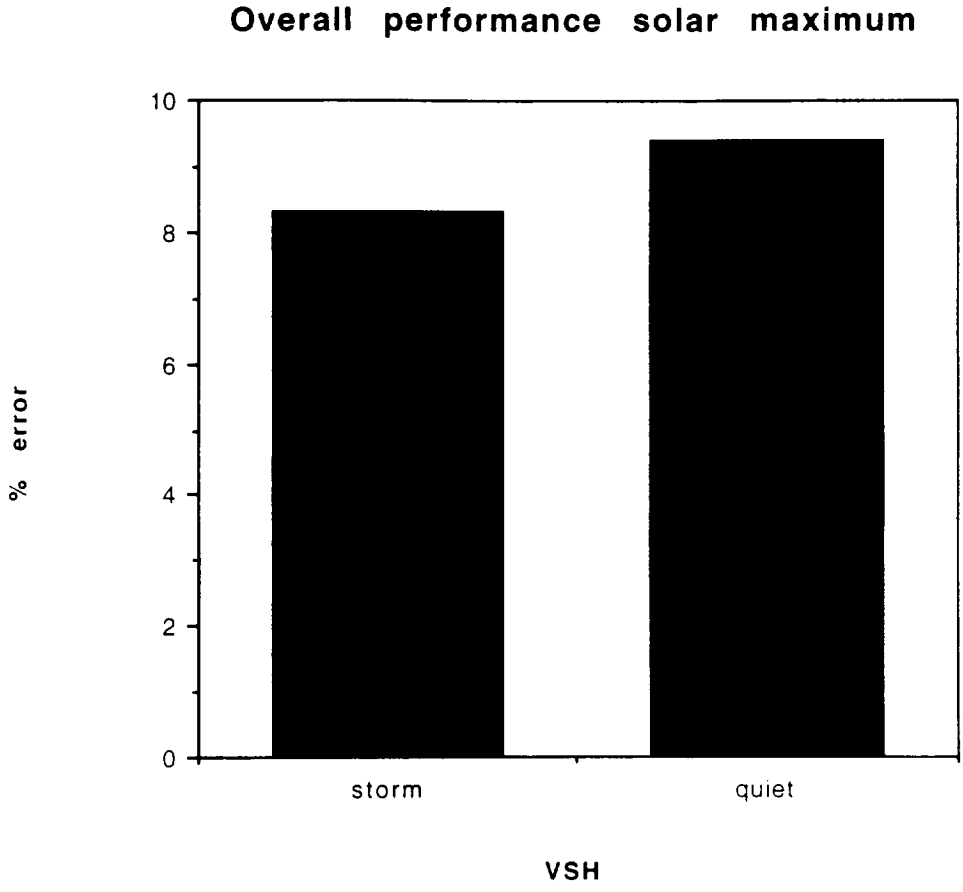

Figure 7. Standard Deviation Comparisons between VSH phase 2 and the time dependent VSH model for the randomly selected days mentioned in the text.

In this test the time-dependent VSH model did 1% better than the non time-dependent version of the VSH model. The relatively small difference between the two versions of the model is attributable to rarity of storm events, even during an active period like the one modeled here. It will become clearer when we look at the Kp trace that performance during storms is superior for the time dependent model.

We also broke the model down into bins by isolating the model performance using a variety of differing geophysical conditions as criteria. Comparisons were then made between the time dependent version of the model and the non time-dependent version to see where differences occurred. The results of these studies are shown in Figures 8 to 11.

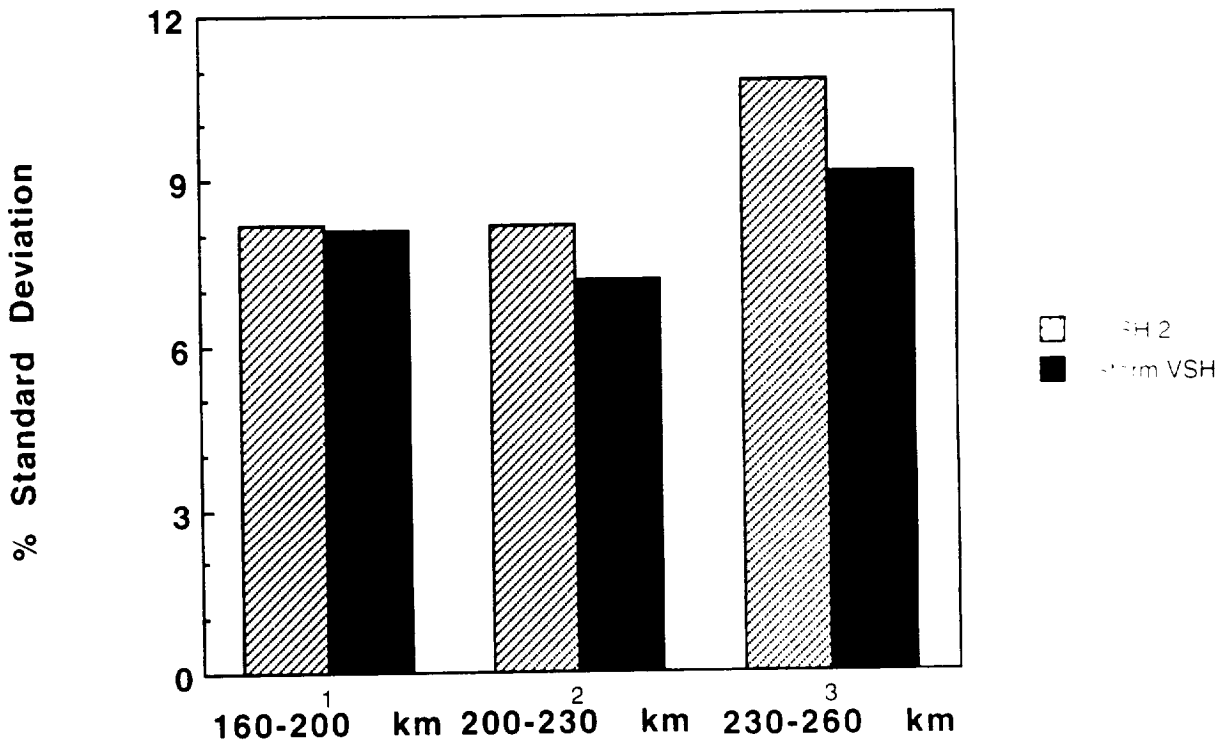

Figure 8. Comparisons between the two versions of the VSH model binned by altitude.

In Figure 8, the altitude plot, the greatest improvement occurs at the highest altitudes (230-260 km), where there is a 2% increase in density specification accuracy from 11% to 9%, but there is not much improvement at low altitudes. Presumably, this large improvement at high latitudes occurs because storm effects are much more dominant at high latitudes. In addition, apogee for this mission occurred near the south pole, so both the high and low altitude bins occur in predominantly polar regions, where the greatest

improvements are expected to lie. The northern bin is at too low an altitude for the densities to be affected as strongly by geomagnetic activity as the other bin.

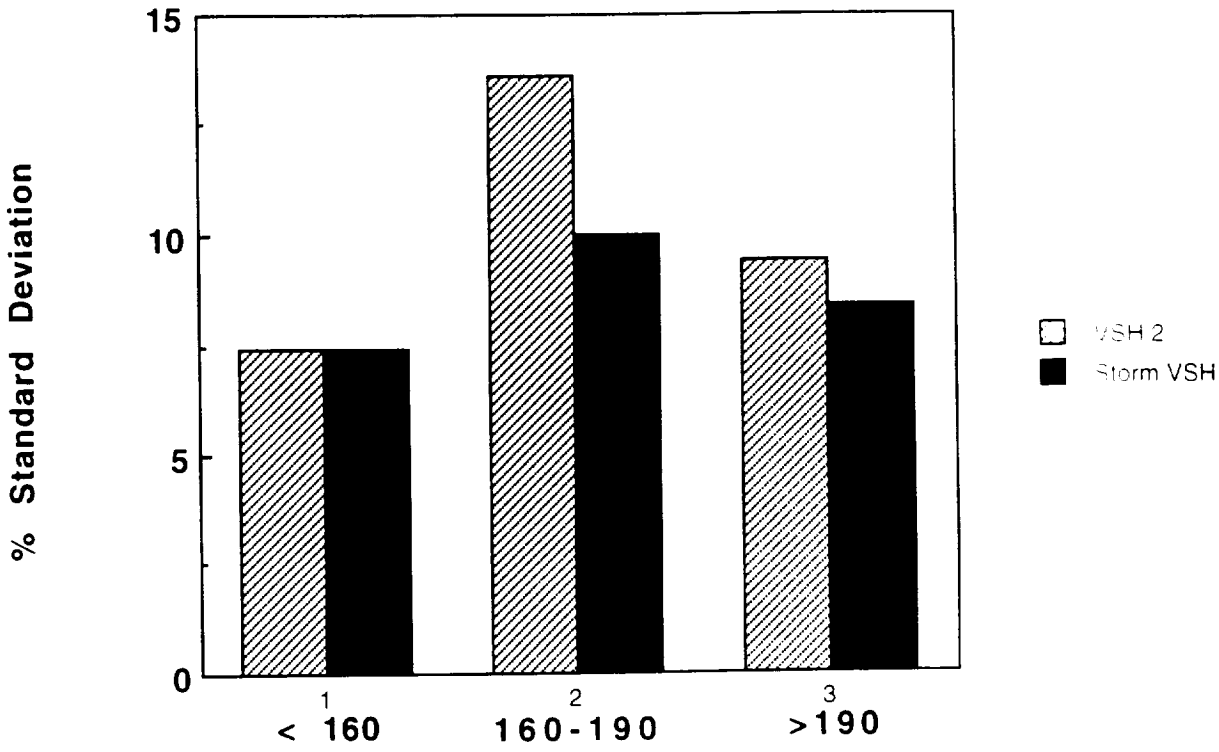

Figure 9. Comparisons between the two versions of the VSH model binned by F10.7.

The F10.7 bins also show marked variations in response to the improvements in geomagnetic forcing representation that occur with the time-dependent version of the model. However, these variations are an artifact of the small sampling size of the F10.7 binning. Because we have only fourteen days of data, we have only fourteen independent F10.7 samples. Both days upon which storms were almost continuous happened during a period when the F10.7 values fell within the middle bin. Thus, there was a marked improvement in the density representation in the middle bin (14-10%) and little improvement in the other two bins.

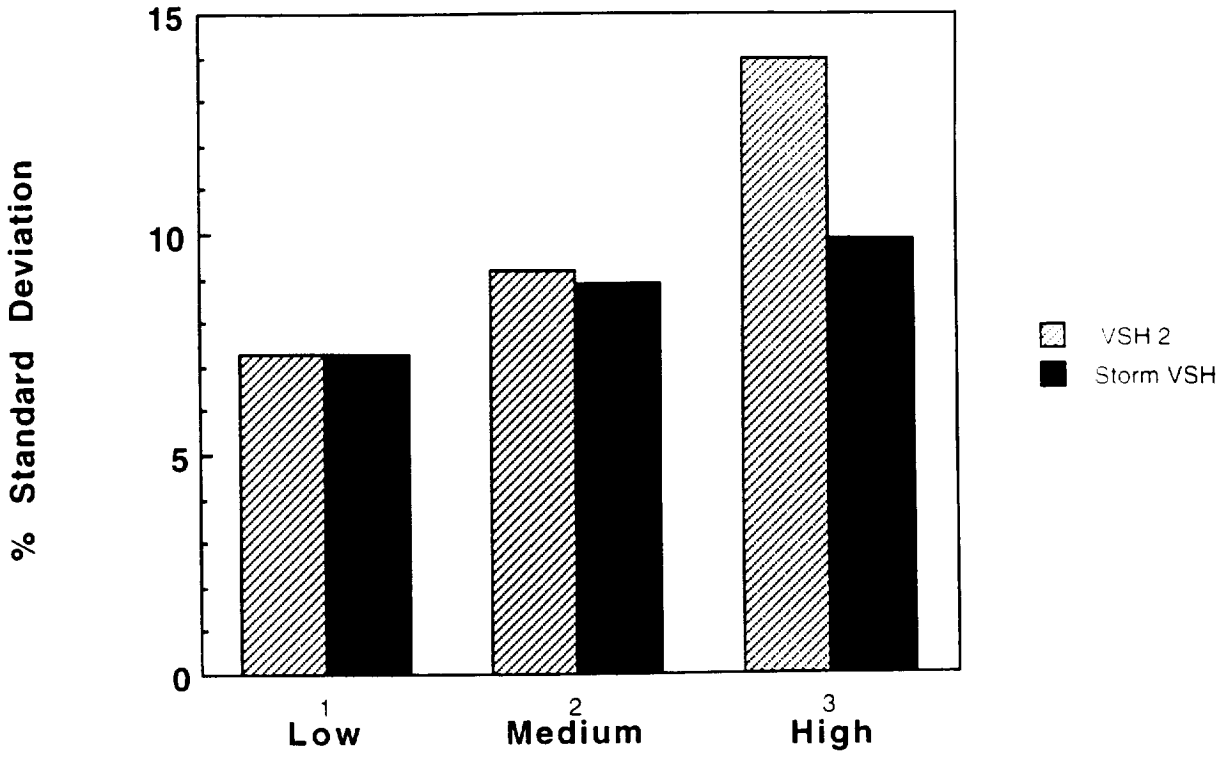

Figure 10. Comparisons between the two versions of the VSH model binned by kp.

Perhaps the most interesting Figure of these four is Figure 10, which shows the improvement of the time-dependent VSH model over the older version at different kp levels. Naturally enough, there is little improvement at low kps, as the time-dependent model does not affect densities in this kp range. However, the time-dependent model should not affect kps in the middle kp range either, yet there is about a 0.5% improvement in this range. Presumably, this difference is due to the time-dependent model's calculation of densities for a recovery period after the cessation of geomagnetic forcing. The largest improvements occur at high kps. Now the errors in the time-dependent model's estimation of density is 9.5%, as opposed to the earlier version of the model, which had an error of 14%. This represents a tremendous improvement in density specification attained by using a true time-dependent model.

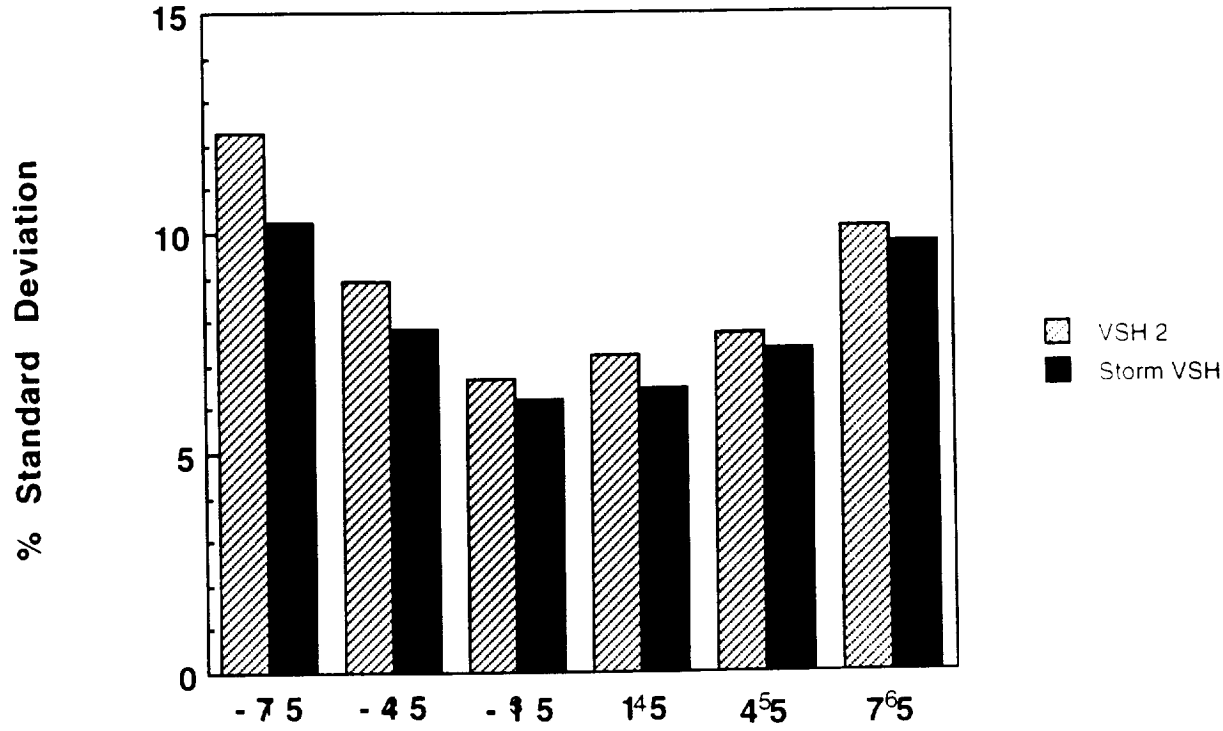

Figure 11. Comparisons between the two versions of the VSH model binned by Latitude.

The last Figure in this suite (11) shows the latitudinal variation of density specification errors. Like the F10.7 and altitude plots, this plot must be treated with a little caution. As we stated earlier, satellite apogee occurred near the southern pole, so the southern latitude bins represent density changes at the highest altitudes, while northern density changes represent those occurring at the lowest altitudes. Therefore, density specification improvements are greatest in the southern high latitudes, where they are of the order of two percent.

. Comparisons between the VSH model and OSS data from AEC (solar minimum nditions)

Comparisons between AE data and the VSH model are more problematical as the data ıd to be pushing the level of reliability that is achieved by the VSH model. The current mparisons are those made with the Open Source neutral mass Spectrometer (OSS).
The data come from all of the long duration storms that occurred during the first year AEC operations. They are detailed in the following table.

ate	Duration	Maximum kp
4080->74081	21 hours	6.667
4082	9 hours	6.0
4093	6 hours	6.0
4108	12 hours	6.0
4186->74187	42 hours	8.667
4204->74205	30 hours	7.0
4286->74291	138 hours (not continuous)	7.0
4315->74316	30 hours	6.3

able. Geomagnetic storms that occurred during the first year of AE-C operations ›r which there was good data coverage.

Unlike the solar maximum case all of the data come from periods in which eomagnetic storms were occurring. Thus, in the following plots, no comparisons have een made with respect to geomagnetic activity as the amount of data available for such mparisons would be slight.

The first comparison is an overall one, made between the "storm" VSH model and the ld non-storm version of the model.

The first such comparison is by local time. Data existed for local times from 0 to 18, but not for local times between 18 and 24, so no bar is given for the last local time band.

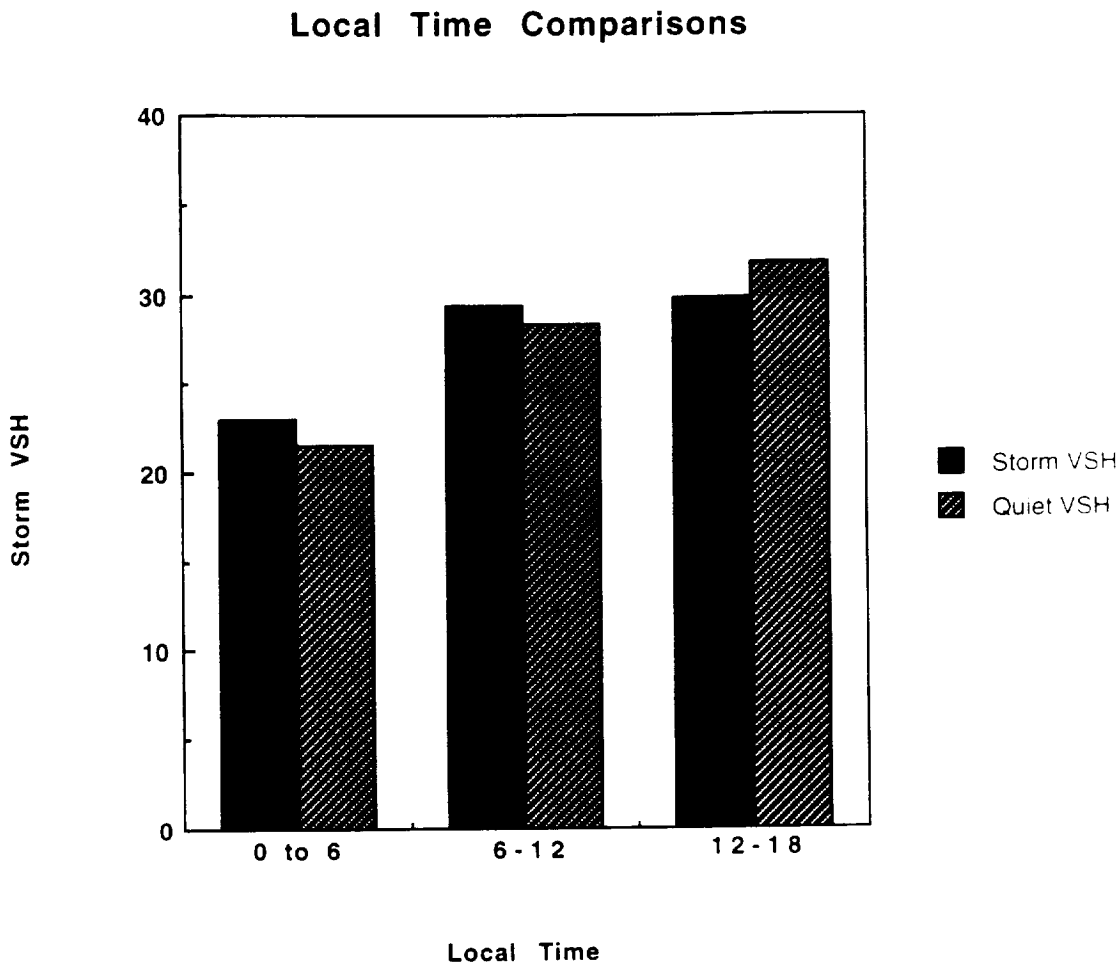

Figure 13. Local time Variations at solar minimum

The largest uncertainty occurs in the afternoon local time band. This problem relates to the nature of the disturbance associated with the geomagnetic storm, and the effects are also affected by latitude variations. During storms the whole thermosphere heats up, but the region during the daytime is particularly affected by changes in the pressure gradient force, and hence by changes in heating by adiabatic expansion and contraction. The NCAR-TIGCM is missestimating these changes during solar minimum conditions, although it does not do so during solar maximum conditions.

The next plot shows the latitudinal comparisons.

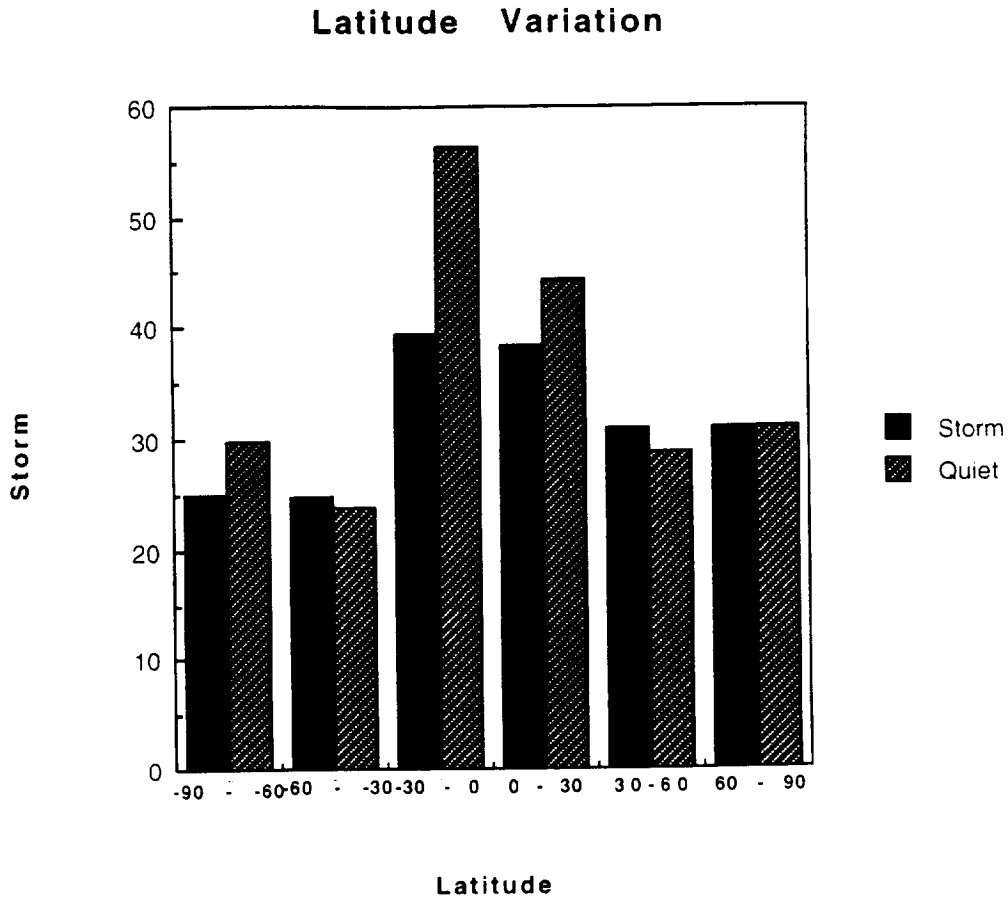

Figure 14. VSH OSS differences in terms of latitude.

Surprisingly, in this plot the greatest uncertainty occurs at low latitudes rather than at the high latitudes where it should be expected during geomagnetic storms. Again this is an indication that the NCAR-TIGCM is missestimating the effects of adiabatic expansion. We will show shortly that the NCAR-TIGCM is in fact underestimating this effect.

The next plot, which shows latitudinal variations, is somewhat less informative.

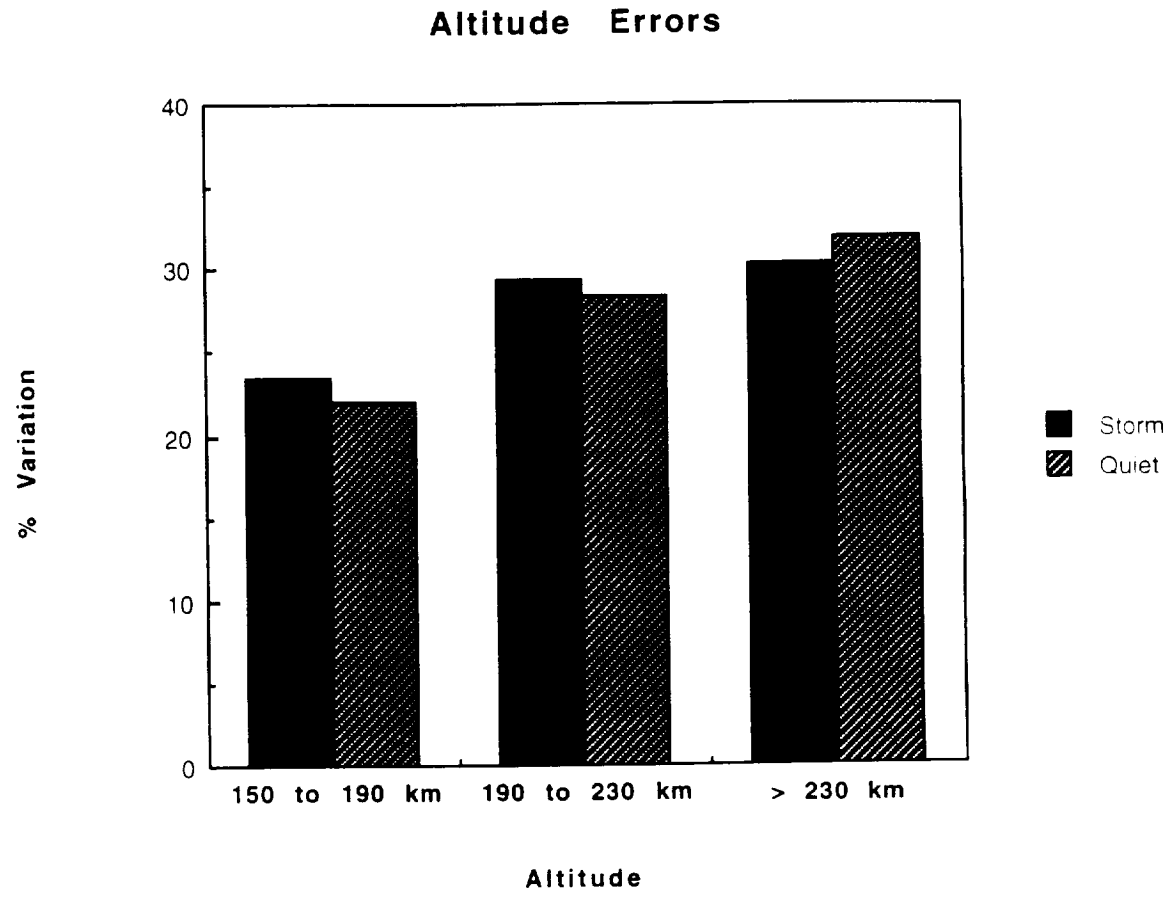

Figure 15. VSH OSS differences in terms of altitude above the Earth's surface.

The density variations are expected to be smaller at lower altitudes where storms cause smaller perturbations. However, there may be another effect insofar as the variations due to latitude and local time may bend back into the altitude variations, due to the relatively small size of the data sample.

Can we determine whether the VSH model is overestimating or underestimating the storm variations? There is an easy way to do this. Instead of determining the variance between the VSH results and the model data, one uses the mean difference. Figure 16 has been developed by doing this.

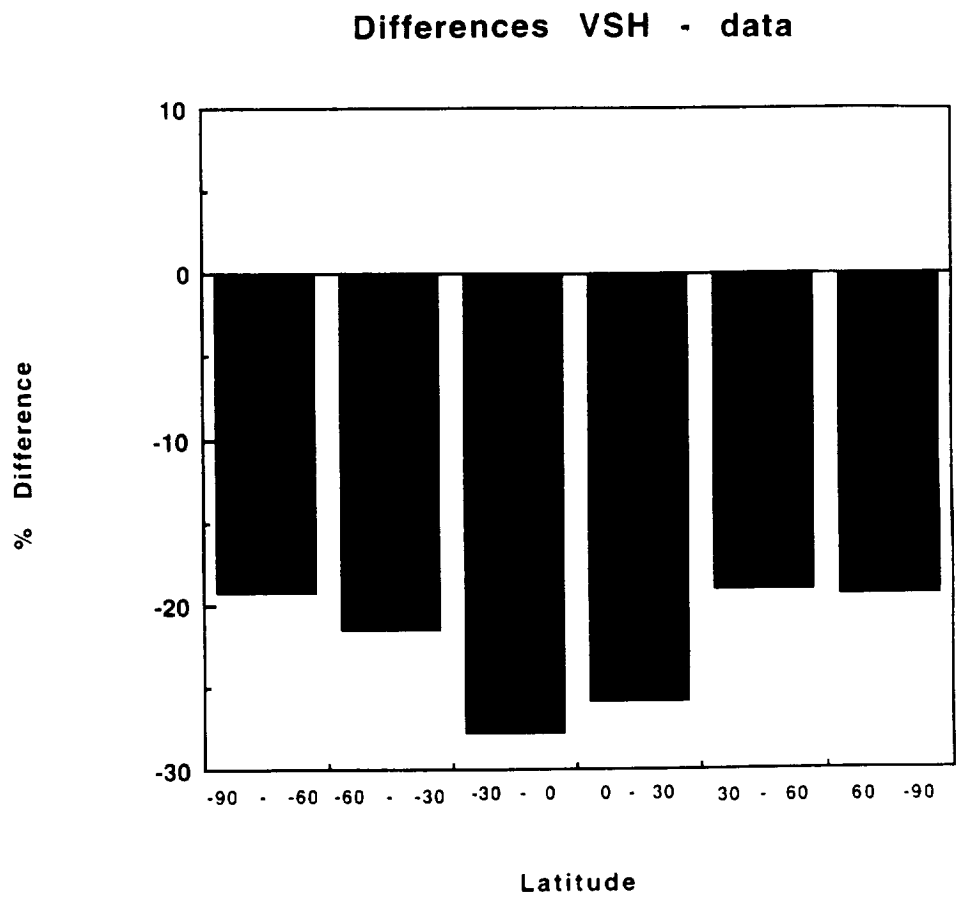

Figure 16.

It is clear that the NCAR-TIGCM is considerably underestimating the density variations that occur during geomagnetic storms, and that this then affects the VSH estimations in turn.

This complication has been corrected in the following manner. Because we are using difference fields, a simple correction factor was applied to the coefficients. The solar minimum storm coefficients were increased by the appropriate amount for each latitude band. These then fold into the equivalent solar maximum storm coefficients by the weighting schemes discussed previously.

11. B_y Considerations: Should B_y Effects be Included

As part of the contract it was proposed that the importance of B_y (The Y component of the IMF) effects should be assessed. Two factors would affect their possible inclusion in the model. The first is obviously whether they are important or not. The second is whether they are sufficiently important to justify inclusion in the model given that there would be a large overhead in terms of model run time and storage requirements. In this section it is shown that, in fact, changes in B_y during storm time are of little importance for all fields apart from the neutral winds, so they have not been included in the VSH model.

The Interplanetary Magnetic Field (IMF) affects the Earth's thermosphere through magnetosphere-ionosphere coupling. Charged particles in the solar wind interact with the Earth's magnetosphere forcing electric fields at high latitudes. These electric fields are altered by the strength, and particularly by the direction of the Interplanetary Magnetic Field. At present the convection pattern for northward IMF is not well enough known to include the results for this condition into models with confidence that it is appropriate. However this is not a large problem for global thermospheric problems, as the effect of the electric fields is minor when B_z is northward, so that approximating northward conditions with very low polar cap potentials is sufficiently accurate for all but the highest latitudes. In terms of general thermospheric studies the more interesting case occurs when B_z is southward (or in certain other circumstances the discussion of which requires a level of complexity which is not appropriate here). In this case the sign of the Y component of the IMF (B_y) becomes important.

Before discussing the effects of B_y on the neutral winds and ultimately the neutral densities further, it is necessary to describe briefly the TIGCM runs that were made to produce these winds. Two model runs are described here. In each case (see Figure 17) the same hemispheric powers and cross cap potentials were used.

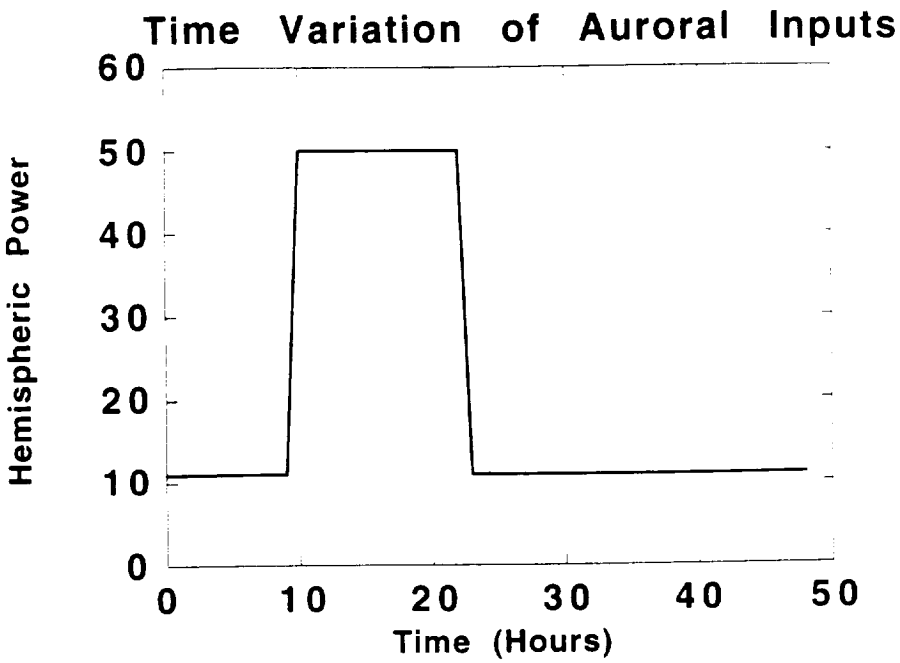

Figure 17

Hemispheric power was increased from 11 to 100 GW between 9 UT and 10 UT. The model was then run for 12 hours with this power. After 22 UT hemispheric power is decreased steadily from 100 GW to 11 GW over an hour. In one case this simulation of a large storm was run for B_y values of -10 nT, in the other case it was run for B_y values of +10 nT.

Figure 18 shows the resultant winds at 18 UT for B_y negative (top) and B_y positive (bottom). These plots are for the southern (summer) hemisphere, and their outer circle occurs at 30 degrees, so they include a large swathe of the middle latitudes.

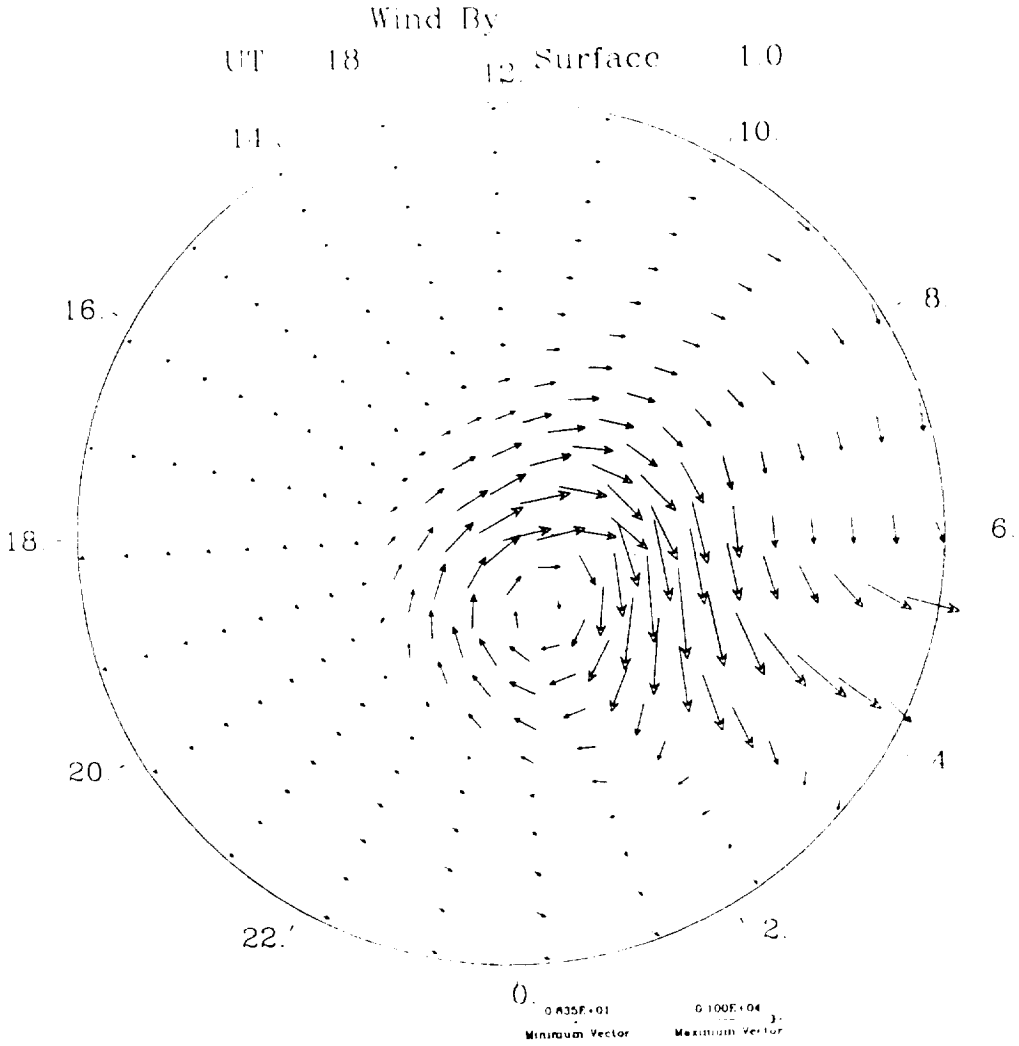

LATITUDE/LOCAL TIME

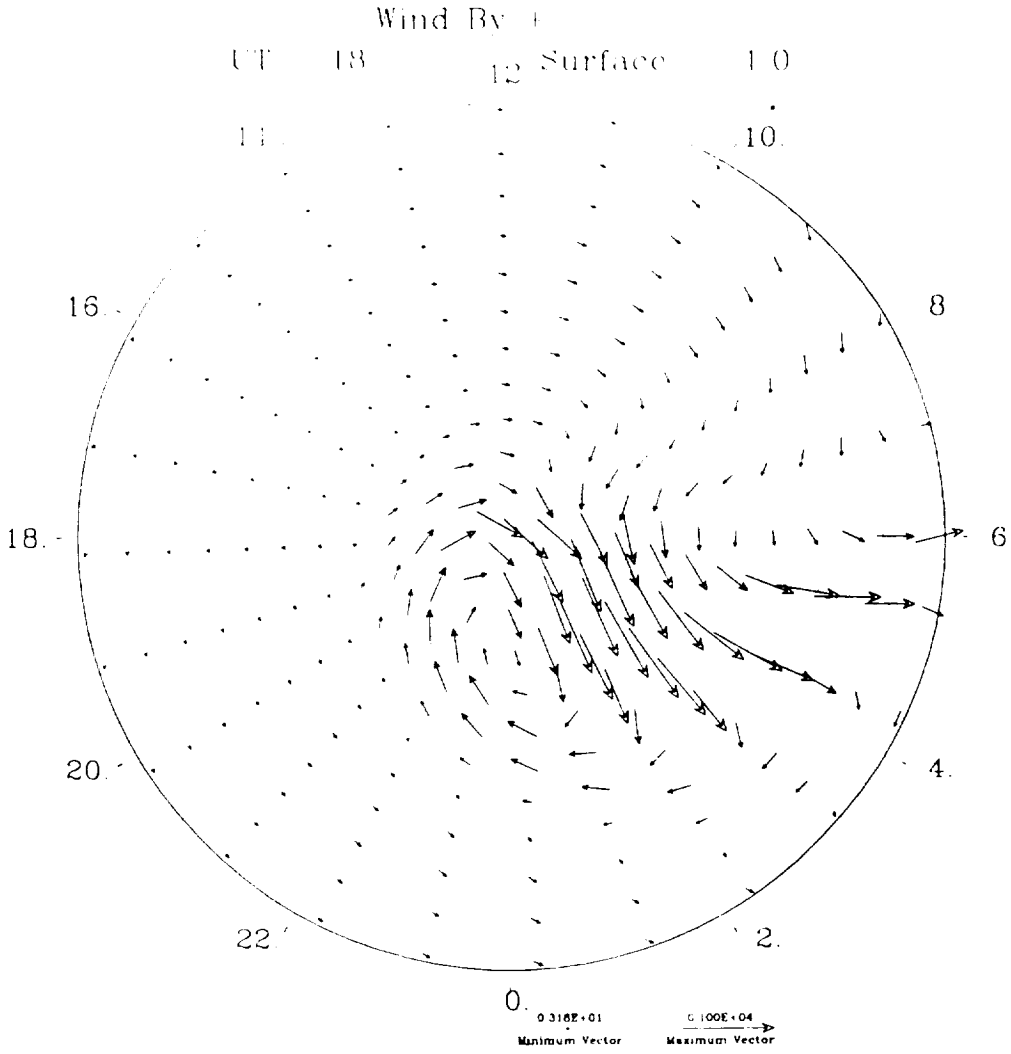

Figure 18

There are clear differences between the two plots. In the main antisunward channel, winds during By positive conditions are rotated by 30 degrees relative to those that occur in B_y negative conditions. The evening convection cell is much better defined during B_y negative conditions than during B_y positive conditions, but the morning convection cell is somewhat evident in B_y positive conditions, but not during B_y negative conditions.

Difference plots of these two conditions are shown in Figure 19.

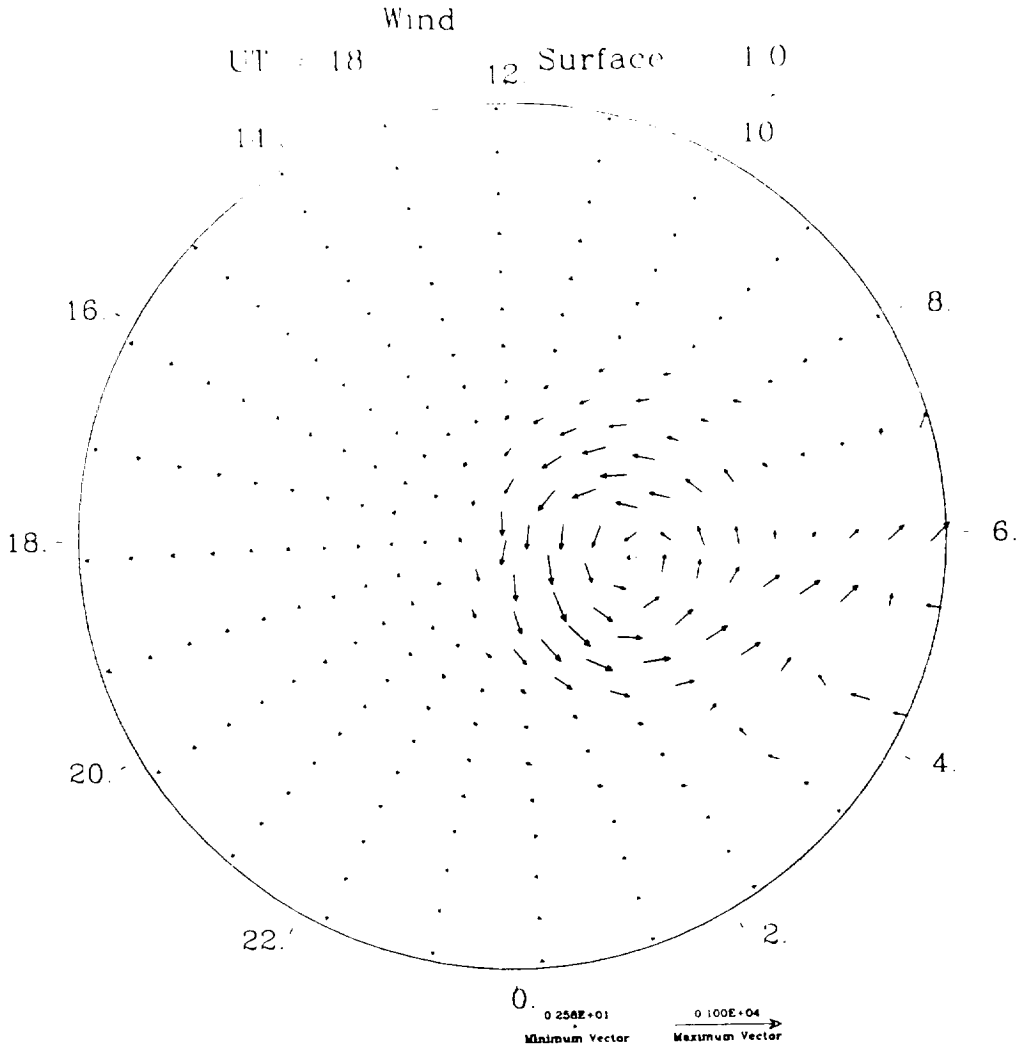

Figure 19

The differences are obtained by averaging the B_y positive and negative data and then subtracting this average from the B_y negative case. The maximum wind differences are of the order of 300 or 400 m/s, quite large values compared with the original wind fields. However these large differences are concentrated in a relatively small area of the high latitudes. As will be shown shortly, these large differences in the winds do not translate into significant differences in the other scalar fields.

Similar plots were worked out for neutral density. This field is closer to the fields for which the VSH model is required. Figure 20 shows the percentage differences that were worked out using the relationship:

$$\text{Percent} = (\text{Dens}_{By+} - \text{Dens}_{ave}) / \text{Dens}_{ave} * 100$$

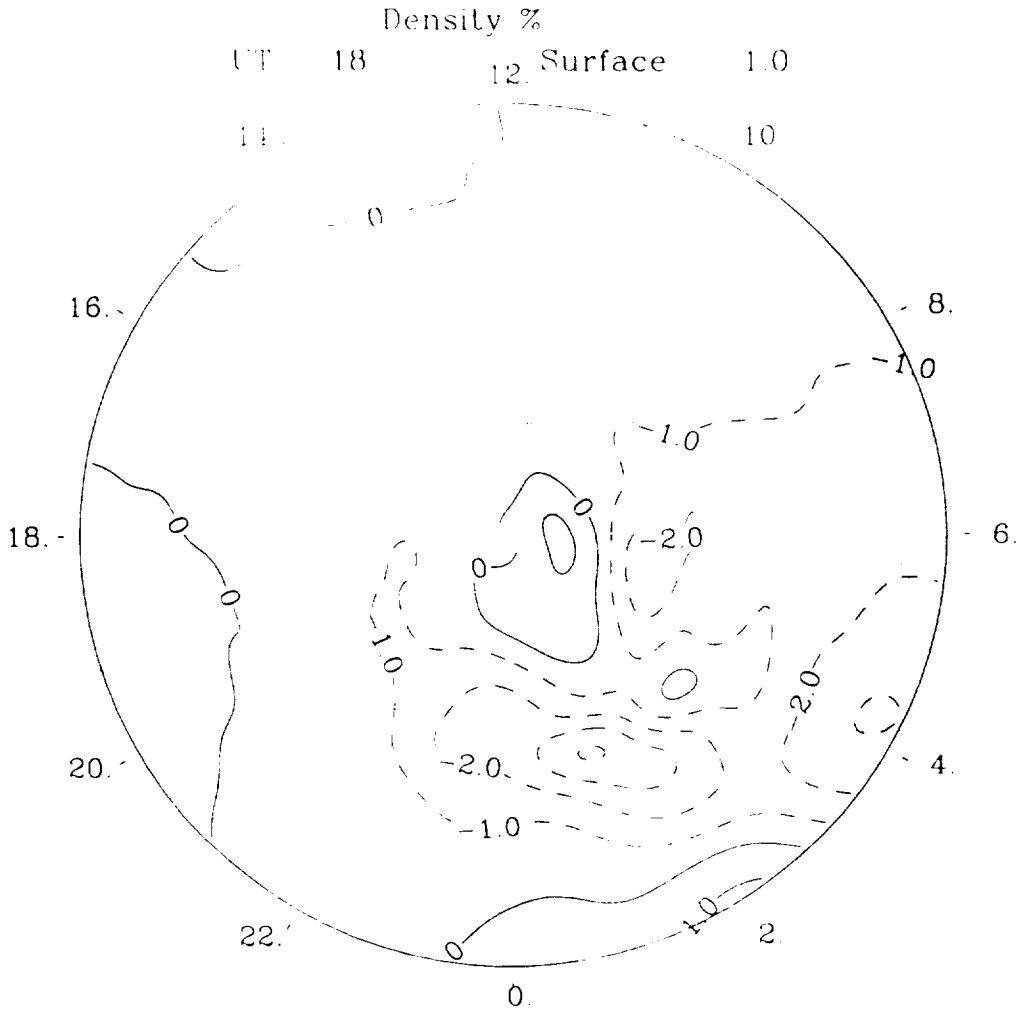

Figure 20

Figure 20 gives these percentage differences in the southern (summer) hemisphere. At this UT, 8 hours after the start of the storm, maximum differences in density are only 4% in the summer hemisphere, and that difference occurs only in a very small area near

midnight. On average density differences between the B_y positive case and the average storm behavior are negligible.

The differences are somewhat larger in winter, but their maximum value is still considerably less than 10% (Figure 21).

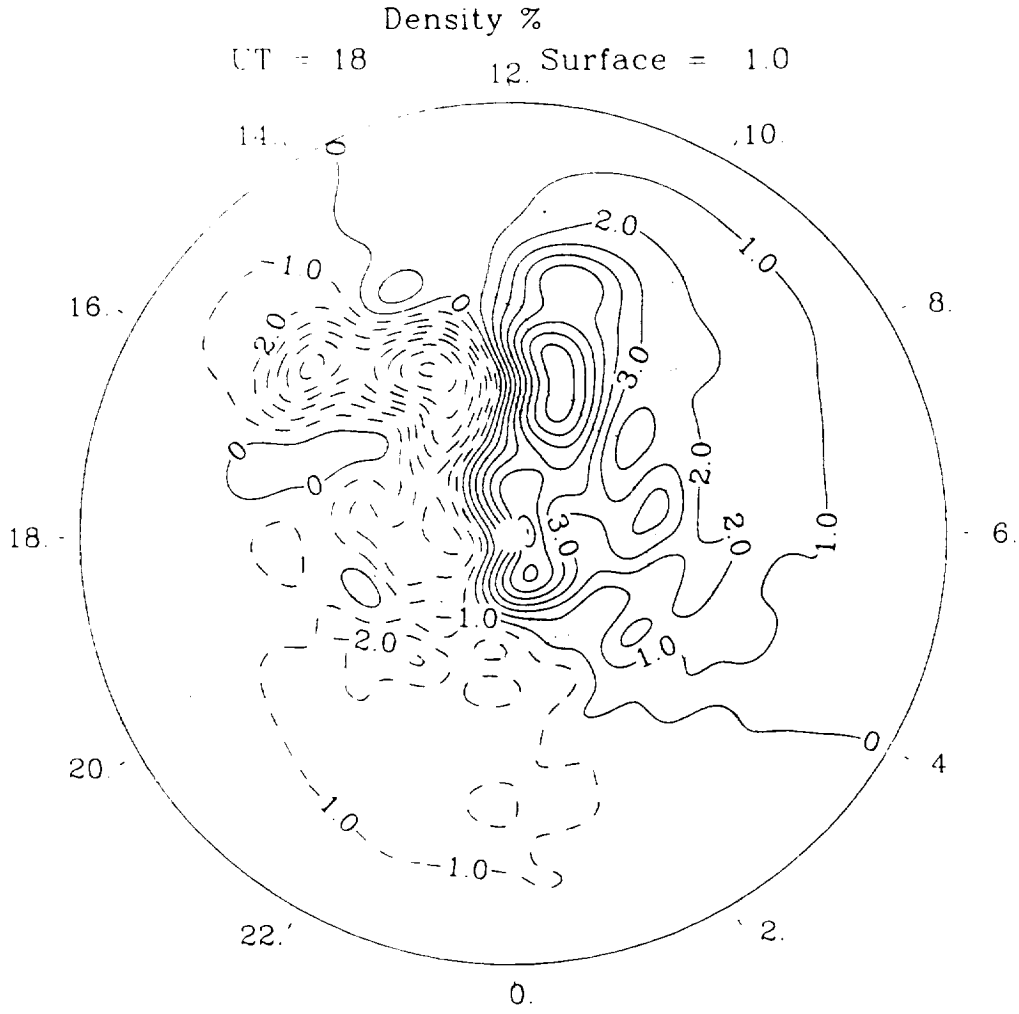

Figure 21

Average values at high latitudes are of the order of about 2%. The maximum changes occur near the "throat" region, the region in which the neutral winds associated with the

convection pattern converge on the dayside of the auroral oval. The asymmetry of the pattern (negative on the left hand side, positive on the right hand side) is due to the different directions of the the antisunward winds in the two extreme cases of B_y, and to the different shapes of the two convection cells for these extremes.

Clearly, at this particular storm time B_y effects are of minor importance in determining density changes. The remaining question is whether these changes can become important at any time during a storm. To test this effect all percentage differences between B_y positive densities and the average density poleward of 60 degrees were averaged for each hour of storm time. The resultant data are plotted here (Figures 22 and 23) in terms of average percentage difference versus time after the storm commenced.

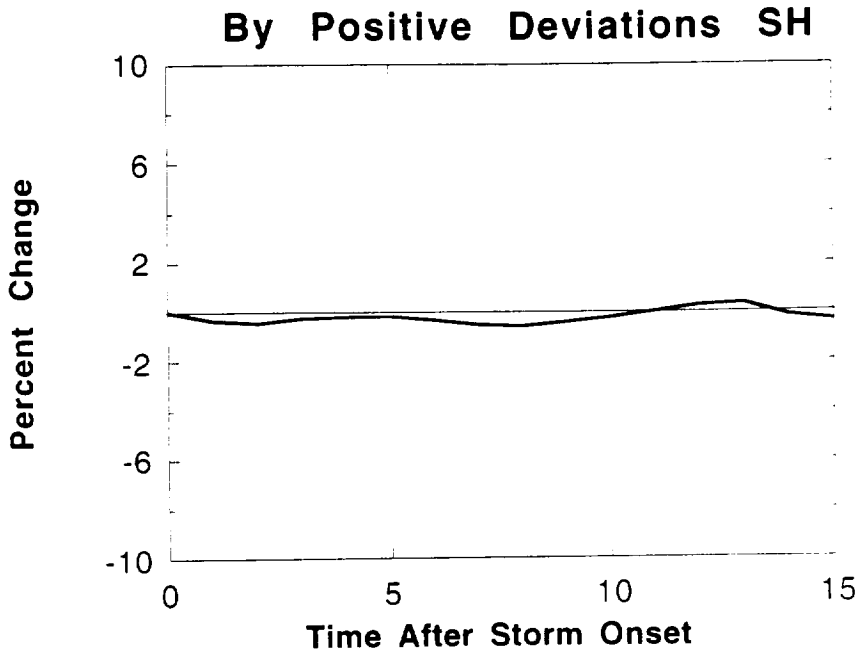

Figure 22

Figure 22 shows the averaged percentage variation of density in the southern (summer) hemisphere for B_y positive conditions during the storm. It can be seen from this diagram that the average variation is very small and that it does not increase greatly (if at all) during the storm (the first 13 hours of the study) or the recovery period. If global or hemispheric averages were used the improved accuracy of the model would be negligible

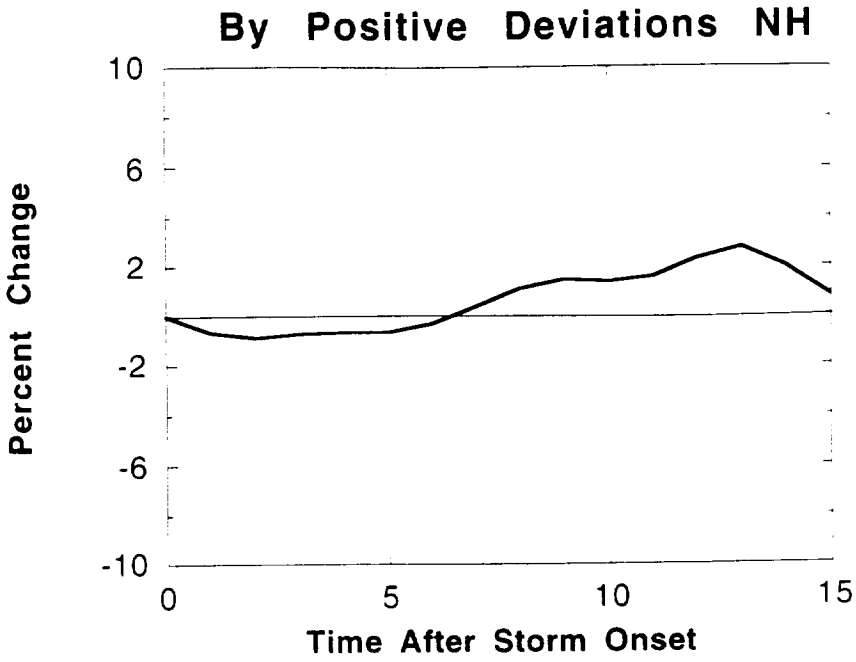

Figure 23

In winter the maximum averaged effect reaches 2% by the end of the storm period. Globally (or hemispherically) this difference is insignificant compared with the very large changes of neutral density (total neutral densities can increase by 100% over the high latitudes during geomagnetic storms and neutral N_2 densities can change by several hundreds of a percent, *Prölss*, 1980).

In this section it has been shown that the changes in density caused by changes in the Y component of the IMF are minor compared with the changes that are caused by geomagnetic storms themselves. Even without considerations of the loss of run time in the model, it is not a useful exercise to include information about the Y component of the IMF in the VSH model, with the possible exception of the case when the model is to be used as a high latitude wind model. Because the model is to be used by NASA primarily as a low latitude density model, B_y effects have not been included in the model that is delivered here. Instructions for running the model are included in the Appendix.

12. REFERENCES.

Burns, A. G. and T. L. Killeen, The equatorial neutral thermospheric response to geomagnetic forcing, Geophys. Res. Lett, 19, 977-981, 1992 a.

Burns, A. G. and T. L. Killeen, Changes of neutral composition in the thermosphere. Adv. Astronaut. Sci., 3, 2295-2312, 1992b.

Burns, A. G., T. L. Killeen and R. G. Roble, Causes of changes in composition calculated using a thermospheric general circulation model, J. Geophys. Res., 94, 3670 - 3686, 1989.

Burns, A. G., T. L. Killeen and R. G. Roble, A simulation of the thermospheric composition changes seen during a geomagnetic storm, Adv. Space Res., 12, (10)253-(10)256, 1992 a.

Burns, A. G., T. L. Killeen and R. G. Roble, Thermospheric heating away from the auroral oval during geomagnetic storms, Can. J. Phys., Can. J. Phys., 70, 544-552 1992 b.

Burrage, M. D., V. J. Abreu, N. Orsini, C. G. Fesen and R. G. Roble, Geomagnetic activity effects on the equatorial neutral thermosphere, J. Geophys. Res., 97, 4177-4187, 1992.

Campbell, I. M. and C. N. Gray, Rate constants for $O(^3P)$ recombination and association with $N(^4S)$, Chem. Phys. Lett., 18, 607-609.

Chiu, Y. T., An improved phenomenological model of ionospheric density, J. Atmos. Terr. Phys., 37, 1563-1570, 1975.

Colegrove, F. D., Atmospheric compositionin the lower thermosphere, J. Geophys. Res., 71, 2227-2236.

Crowley, G., B. A. Emery, R. G. Roble, H. C. Carlson, Jr. and D. J. Knipp, Thermospheric dynamics during September 18-19, 1984, 1, model simulations, J. Geophys. Res., 94, 16925-16944, 1989.

Dickinson, R. E., E. C. Ridley and R. G. Roble, A three-dimensional general circulation model of the thermosphere, J. Geophys. Res., 86, 1499-1512, 1981.

Dickinson, R. E., E. C. Ridley and R. G. Roble, Thermospheric general circulation with coupled dynamics and composition, J. Atmos. Sci., 41, 205-219, 1984.

Feldstein, Y. I. and Yu. I. Galperin, The auroral luminosity structure in the high-latitude upper atmosphere: Its dynamics and relationship to the large-scale structure of the earth's magnetosphere, Rev. Geophys. Space Phys., 23, 217-276, 1985.

Fesen, C. G. and R. G. Roble, Simulations of the September 1987 lower thermospheric tides withe the National Center for Atmospheric Research Thermosphere-Ionosphere General Circulation Model, J. Geophys. Res., 96, 1173-1180, 1991.

Fuller-Rowell, T. J. and D. Rees, A three-dimensional time-dependent global model of the thermosphere, J. Atmos. Sci., 37, 2545-2567, 1980.

Fuller-Rowell, T. J. and D. Rees, A three-dimensional time dependent simulation of the global dynamical response of the thermosphere to a geomagnetic substorm, J. Atmos. Terr. Phys., 43, 701-721, 1981.

Fuller-Rowell, T. J. and D. Rees, Derivation of a conservation equation for mean molecular weight for a two-constituent gas within a three-dimensional, time-dependent model of the thermosphere, Planet. Space Sci., 31, 1209-1222, 1983.

Fuller-Rowell, T. J., S. Quegan, D. Rees, R. J. Moffett and G. J. Bailey, Interactions between neutral thermospheric composition and the polar ionosphere using a coupled ionosphere-thermosphere model, J. Geophys. Res., 92, 7744-7748, 1987.

Fuller-Rowell, T. J., M. V. Codrescu, R. J. Moffett and S. Quegan, Response of the thermosphere and ionosphere to geomagnetic storms, J. Geophys Res., 99, 3893-3914, 1994.

Hays, P. B., T. L. Killeen, N. W. Spencer, L. E. Wharton, R. G. Roble, B. E. Emery, T. J. Fuller-Rowell, D. Rees, L. A. Frank and J. D. Craven, Observations of the dynamics of the polar thermosphere, J. Geophys. Res., 89, 5597-5612, 1984.

Hedin, A. E., P. Bauer, H. G. Mayr, G. R. Carignan, L. H. Brace, H. C. Brinton, A. D. Parks and D. T. Pelz, Observations of neutral composition and related ionospheric variations during a magnetic storm in February 1974, J. Geophys. Res., 82, 3183-3189, 1977.

Heelis, R. A., J. K. Lowell and R. W. Spiro, A model of the high-latitude ionospheric convection pattern, J. Geophys. Res., 87, 6339-6345, 1982.

Hinteregger, H. E., Representation of solar EUV fluxes for aeronomical applications, Adv. Space Res., 1, 39-52, 1981.

Johnston, H. S., Gas Phase Reaction Kinetics of Neutral Oxygen Species, NBS-NSRSDS-20, US Government Printing Office, Washington, D. C.

Killeen, T. L., R. G. Roble, and N. W. Spencer (1987) A computer model of global thermospheric winds and temperatures, Adv. Space Res., 7, 207-215.

Maeda, S., T. J. Fuller-Rowell and D. S. Evans, Zonally averaged dynamical and compositional response of the thermosphere to auroral activity during September 18-24, 1984, J. Geophys Res., 94, 16869-16884, 1989.

Matsushita, S., A study of the morphology of ionospheric storms, J. Geophys. Res., 64, 305-321, 1959.

Mayr, H. G., I. Harris, F. Varosi and F. A. Herrero, Global excitation of wave phenomena in a dissipative multiconstituent medium. 2. Impulsive perturbations in the Earth's thermosphere, J. Geophys. Res., 89, 10961-10986, 1984.

Ponthieu, J.-J., T. L. Killeen, K.-M. Lee, G. R. Carignan, W. R. Hoegy, and L. H. Brace, Ionosphere-thermosphere momentum coupling at solar maximum and solar minimum from DE-2 and AE-C data, Physica Scripta, 37, 447-454, 1988.

Porter, H. S., H. G. Mayr and A. E. Hedin, An analytic formulation for heating source memory in the thermospheric composition, J. Geophys. Res., 86, 3555-3560, 1981.

Prölss, G. W., Magnetic storm associated perturbation of the upper atmosphere: recent results obtained by satellite-borne gas analyzers, Rev. Geophys. Space Phys., 18, 183-202, 1980.

Richmond, A. D., M. Blanc, B. A. Emery, R. H. Wand, B. G. Fejer, R. F. Woodman, S. Ganguly, P. Amayenc, R. A. Behnke, C. Calderon, and J. V. Evans, An empirical model of quiet-day ionospheric electric fields at middle and low latitudes, J. Geophys. Res., 85, 4658, 1980.

Richmond, A. D., E. C. Ridley and R. G. Roble, A Thermosphere/Ionosphere General Circulation Model with coupled electrodynamics, Geophys. Res. Lett., 19, 601-604, 1992.

Roble, R. G. and Ridley, E. C., An auroral model for the NCAR thermospheric general circulation model (TGCM), Ann. Geophysicae, 5A, 369-382, 1987.

Roble, R. G. and E. C. Ridley, A thermosphere-ionosphere-mesosphere-electrodynamics general circulation model (time-GCM): equinox solarcycle minimum simulations (30-500 km), Geophys. Res. Lett., 21, 417,420, 1994.

Roble, R. G., R. E. Dickinson and E. C. Ridley, Global circulation and temperature structure of thermosphere with high-latitude plasma convection, J. Geophys. Res., 87, 1599-1614, 1982.

Roble, R. G., B. A. Emery, R. E. Dickinson, E. C. Ridley, T. L. Killeen, P. B. Hays and G. R. Carignan, Thermospheric circulation, temperature, and compositional structure of the southern hemisphere polar cap during October-November 1981, J. Geophys. Res., 89, 9057-9068, 1984.

Roble, R. G., E. C. Ridley and R. E. Dickinson, On the global mean structure of the thermosphere, J. Geophys. Res., 92, 8745-8758, 1987.

Roble, R. G., T. L. Killeen, N. W. Spencer, R. A. Heelis, P. H. Reiff and J. D. Winningham, Thermospheric dynamics during November 21-22, 1981: Dynamics Explorer measurements and thermospheric general circulation model predictions, J. Geophys. Res., 93, 209-225, 1988.

Roble, R. G., E. C. Ridley, A. D. Richmond and R. E. Dickinson, A coupled thermosphere/ionosphere general circulation model, Geophys. Res. Lett., 15, 1325-1328, 1988.

Spiro, R. W., P. H. Reiff and L. J. Maher, Jr., Precipitating electron energy flux and auroral zone conductances - An empirical model, J. Geophys. Res., 87, 8215-8227, 1982.

Swarztrauber R.N. (1981) The approximation of vector functions and their derivatives on the sphere, SIAM J. Numer. Anal., 18, 934-949.

Thiebaux, H.J. and M.A. Pedder (1987) Spatial Objective Analysis, Academic Press, London, 295 pp.

Torr, M. R. , D. G. Torr and H. E. Hinteregger, Solar flux variability in the Schumann-Runge continuum as a function of solar cycle, J. Geophys. Res., 85, 6063-6068, 1980.

Whalen, J. A., A quantitative description of the spatial distribution and dynamics of the energy flux in the continuous aurora, J. Geophys. Res., 88, 7155-7169, 1983.

Appendix 1

VSH MODEL DOCUMENTATION

VERSION 3.0

Space Physics Research Laboratory
The University of Michigan

December 1, 1997

PREFACE

This manual is divided into four sections. Part I provides an overview of the capabilities of VSH. This part is oriented towards all users of VSH and provides the minimum information needed by an end user. Part II details how a FORTRAN program would be written to access the VSH routines. It includes examples of main programs. Part III is a technical description of the underlying atmospheric physics and mathematical equations used in the VSH model. It is most useful for space scientists and others who are interested in the underlying science that went into the development of the VSH model. The final section is directed towards a systems analyst or systems administrator. It provides information on storage, run-time requirements, and installation.

TABLE OF CONTENTS

APPENDIX

PART I: USER'S GUIDE

CHAPTER 1: OVERVIEW

1 *Description*

The VSH (Vector Spherical Harmonic) Model is a computer subroutine that provides a description of the composition and dynamics of the thermosphere (Killeen, et al, 1987). It is capable of integrating real-time data with high-accuracy computer simulations to produce a hybrid model of the thermosphere.

If the user wishes to run VSH, he or she specifies values for time, location, and the prevailing geophysical conditions. With this input, the following atmospheric variables may be obtained:

COMPOSITION
Densities: O, O_2, N_2, H, electron, O^+, total mass
Mixing ratios: O, N_2, O_2

WINDS
Neutral: zonal, meridional, vertical
Ion: zonal, meridional

TEMPERATURE
Neutral, ion

PRESSURE

Two types of input are used to drive the model: the coefficient library and real-time data. The coefficient library contains the output of a large number of runs from a general circulation model of the thermosphere and ionosphere (the NCAR-TIGCM). The real-time data consists of location, time, solar flux and magnetic activity indices, as well as any composition, density, and/or wind information as obtained by satellite measurement.

The general VSH approach is to use the real-time information as a refinement to the computer simulations. In this sense, the satellite data is optional.

VSH can also access the MSIS (Hedin, 1987) empirical model of the upper atmosphere. If a VSH user requests an altitude that is out of range of the TIGCM, the desired information is obtained from the MSIS model. VSH can be called with altitudes up to 1500 km, although it relies upon MSIS to provide density and composition data above about 500 km. Similarly, VSH can be called for altitudes as low as 90 km, however, MSIS is used below 100 km, and a mix of MSIS and VSH results are used between 100 and 110km. MSIS is also called to obtain the H density at all altitudes, as this variable is not provided in the TIGCM.

PART II: PROGRAMMER'S REFERENCE

CHAPTER 2: WRITING A PROGRAM TO CALL VSH

1. *Input/Output variables*

To call the VSH subroutines, use the following (or similar) statement:

CALL VSH(OUTPUT,USING,GLON,GLAT,ALT,UT,JDAY,F107A,F107,AP,APHIST,STFLAG,BYIMF)

OUTPUT VARIABLES:

Name	Type	Description	Units
OUTPUT (25)	REAL	The array of output variables	
		1) Zonal neutral wind(U) (positive eastward)	[illegible]
		2) Meridional neutral wind(V) (positive northward)	[illegible]
		3) Neutral temperature(T)	K
		4) Zonal ion drift (Ui)	[illegible]
		5) Meridional ion drift(Vi)	[illegible]
		6) Pressure ($5x10^{-10}$ *exp(-Z) bars)	
		7) Vertical neutral wind(W)	[illegible]
		8) Atomic oxygen mass mixing ratio	
		9) Mass density	[illegible]
		10) Electron density	[illegible]
		11) O+ density	[illegible]
		12) Ion temperature	K
		13) Molecular oxygen mass mixing ratio	
		20) Atomic oxygen density	[illegible]
		21) Molecular oxygen density	[illegible]
		22) Molecular nitrogen density	[illegible]
		23) Hydrogen density	[illegible]
		24) Molecular nitrogen mass mixing ratio	

(Variables 14-19, and 25 are reserved for future use.)

INPUT VARIABLES:

Name	Type	Description	Units
USING(25)	LOGICAL	An array of 25 logical variables (.true. or .false.) corresponding to each of the above 25 variables. Set a value to .false. to eliminate calculation of that variable (to reduce computation time). Set all desired corresponding output variables to .true.	
GLON	REAL	Geographic longitude	(degrees)
GLAT	REAL	Geographic latitude (-90 to +90)	(degrees)
ALT	REAL	Altitude (90 - 1500 km)	(km)
JDAY	INTEGER	Julian Day (e.g. 324)	
F107A	REAL	Previous 90-day average F10.7 solar flux (50-350)	
F107	REAL	F10.7 value of solar flux (50-350)	
AP	REAL	3-hr ap index (2-80)	
APHIST(8)	REAL	8*3-hr ap index (2-100) from the day prior to the UT time needed. This array is entered in the time sequence of the ap data	
STFLAG	LOGICAL	A flag to switch the storm time VSH flag on or off. If it is .TRUE. the storm VSH is called.	
BYIMF	REAL	The value of the Y component of the IMF. This is not implemented at the moment and should be set equal to zero.	

Alternative Inputs:

1. PRESSURE

In lieu of specifying an altitude, a constant pressure surface can be entered. This option is invoked by specifying a value of ALT between -5.5 (bottom) and +4.5 (top). OUTPUT(6) then outputs the altitude (km) of the inputed pressure.

Alternatively, in lieu of specifying an altitude, a log density may be specified. This option is invoked by entering a natural logarithm between -18 (corresponding to a density of 10^{-8}) and -41 (corresponding to a density of 10^{-18}). OUTPUT(6) then outputs the altitude (km) of the inputed density.

2. TIGCM RUN #

In lieu of specifying the geophysical parameters JDAY, F107A, F107, and AP, a specific TIGCM run can be selected by setting JDAY= -run#, where run# is a number 1 - 38. When this option is selected, the F107A,F107, and AP selections are overridden. For example, JDAY= -25 would select run #25. Descriptions of TIGCM runs are given in Chapter 7 of this manual. Note that this option does not work correctly if STFLAG is .TRUE.

Optional Data Statement Inputs:

Name	Type	Description
IRES	INTEGER	Controls resolution level of model. For IRES = 1 model is much faster, but less accurate. For IRES = 5, model is slower, but more accurate. The default value for IRES is 4. (refer to chapter 8.)

This can be input by including the common block RESO in the driver program, i.e., COMMON/RESO/IRES

2 *Linking VSH with a main program*

To use the VSH module a main driver program must be written, compiled and then linked with the VSH subroutines and libraries: VSH, STORM, VSHIMF VSHLIB, MSIS. On a VAX, the appropriate command for linking these files is:

LINK *PROGRAM,VSH,STORM,VSHIMF,VSHLIB,MSIS*

where PROGRAM is the name of your main program.

On UNIX, the appropriate sequence of commands is:

f77 vsh.
f77 vshlib.f
f77 storm.f
f77 vshimf.f
f77 msis.f
f77 gws3.f
f77 <your program>.f vsh.o storm.o vshimf.o vshlib.o msis.o gws3.o

where <your_program> is the name of your main program. VSH can then be run by typing
a.out
where a.out is the final executable image

3 *Sample Main Programs*

Two sample main programs that call VSH are shown below. The first program generates a polar wind field and is similar to the SAMPLE program that is included with VSH. The second program compares the total mass density with that obtained from a satellite pass.

```
      PROGRAM WINDS
C  Creates a polar wind field
      DIMENSION OUTPUT(25)
      LOGICAL USING(25)
      LOGICAL STFLAG
      REAL APHIST(8)
      DATA USING/2*.TRUE.,23*.FALSE./
      DATA STFLAG/.TRUE./
      DATA ALT/300/, UT/5/, F107A/140/,F107/180/, AP/11/, JDAY/182/, BYIMF/0./
      DO I = 1,8,1
        APHIST(I)=11.
        IF(I .GT. 6.)APHIST(I) = 50.
      ENDDO
      OPEN (15, NAME= WINDS.DAT, STATUS= 'NEW')
      WRITE (15,*) 'LATITUDE LONGITUDE      U          V'
      DO 200 LAT= 40,50,5
            DO 100 LONG= 90,180,30
                CALL VSH (OUTPUT, USING, FLOAT(LONG), FLOAT(LAT), ALT,
     1                                UT, JDAY, F107A, F107, AP,APHIST,STFLAG,
     2                                BYIMF)
              WRITE (15,900) LAT, LONG, OUTPUT(1), OUTPUT(2)
  100       CONTINUE
```

```
200     CONTINUE
        STOP
900     FORMAT (2I9,2F8.1)
        END

        PROGRAM DENSTRAK
C  Calculate density along a satellite orbit
        DIMENSION OUTPUT(25)
        LOGICAL USING (25)
        LOGICAL STFLAG
        REAL APHIST(8)
        DATA STFLAG/.TRUE./, BYIMF/0./

        REAL LAT,LONG
        DATA USING /8*.FALSE.,.TRUE.,16*.FALSE./

        OPEN (1, FILE= 'SAT.DAT',STATUS= 'OLD')
        OPEN (15, FILE='DENS.DAT', STATUS= 'NEW')
        WRITE (15,*) ' UT  LAT     LONG   ALT   SAT. DENS.   VSH DENS'
        DO I = 1,8,1
          APHIST(I)=11.
          IF(I .GT. 6.)APHIST(I) = 50.
        ENDDO
        DO 1000 I= 1,1000
          READ (1,5000,END=2000) JDAY,UT,LAT,LONG,ALT,DEN, F107A, F107, AP
          CALL VSH(OUTPUT, USING, LONG, LAT, ALT, UT, JDAY, F107A, F107, AP,
     1              APHIST,STFLAG,BYIMF)
          WRITE  (15,3000) UT, LAT,LONG,ALT,DEN,OUTPUT(9)
1000    CONTINUE
2000    CONTINUE

        STOP
3000    FORMAT (F5.1,F6.1,F7.1,F7.1,E10.3,E10.3)
5000    FORMAT (I4,F6.1,F7.1,F7.1,F7.1,3E10.3)
        END
```

4 *Hints to reduce computational time*

When VSH is used to generate a global or regional field of values (as is the case with the sample program SAMPLE), the latitude loop should always be outside of the longitude loop. This will eliminate the need to recalculate the basis functions (refer to ch. 6). That is, the basis functions are internally recomputed each time the latitude has changed from the previous call. It is to your advantage to lump all calls with the same latitude in succession.

For testing purposes, specifying a specific TIGCM run (or the geophysical parameters of a specific run) will reduce the number of coefficient files to be read in, and hence also reduce the computation time.

The parameter IRES within VSH enables users to sellect a faster, although less accurate, version of VSH. There are five levels of speed, with 1 being the fastest, least accurate level, and 5 being the slowest, most accurate level. The following table gives the average tradeoff between accuracy and speed for different values of IRES. Refer to chapter 6 for more details on the accuracy / speed tradeoff.

CHAPTER 3: COEFFICIENT LIBRARIES

There are currently thirteen variables contained in the main coefficient libraries:

1. Neutral wind - divergent component
2. Neutral wind - rotational component
3. Neutral temperature
4. Ion drift - divergent component
5. Ion drift - rotational component
6. Height of pressure surface
7. Vertical velocity
8. O mixing ratio
9. Mean molecular weight / temperature
10. Electron density
11. O^+ Density
12. Ion Temperature
13. O_2 mixing ratio

These thirteen fields are used to compute 13 of the variables that are available for output. The remaining 5 output fields are derived fields or are obtained from MSIS. (Currently only 18 of the 25 variables are used.) The same 13 variables are contained in both the storm (stvar) and IMF (byvar) coefficient libraries.

CHAPTER 4: VSH PROGRAM DESCRIPTION

1 *Program Design*

The VSH model consists of a set of subroutines and does not contain a main FORTRAN program (other than the SAMPLE program). Therefore, a main driving program must be written for VSH to become operational.

Upon each call to the primary VSH subroutine, the following algorithm is carried out via a series of subroutine calls. The name of each subroutine is listed below followed by its purpose. Each of the indicated subroutines is called from VSH3BY, STORM or VSHIMF, the primary or controlling subroutines.

1. VSHSOLVE
   Solves for a specific field. Calls main computational and ingestion programs

2. VALIDATE
   Ensures that all needed variables have been assigned values. For example, if geometric height is input pressure coefficient file is also required.

3. WHATSNEW
   Determines whether any of the following have changed since the last call: latitude, time, altitude, geophysical parameters, required variables.

4. COEFFSEL
   Determines which coefficient files are to be read and takes weighted averages of coefficient files if necessary.

5. TRUNCIN
   Reads in the truncation structure that is used in the variable resolution processing of VSH coefficients

6. COEFFIN
   If geophysical parameters or any variables have changed the applicable coefficients are read in. Applies height modifier to altitude versus pressure level to allign TIGCM global average to MSIS global average. Also modifies TIGCM global average to agree with global averages obtained from the SETA2 satellite.

6. TIMETR
   If coefficients have changed or if the requested time has changed, a Fourier time synthesis is performed for the requested time for each variable, altitude, and zonal and meridional wavenumber.

7. BASIS
   If latitude has changed, then for the requested latitude, BASIS finds the values of the vector spherical harmonics P, V, and W for each zonal and meridional wavenumber.

8. GETPRESS
   Converts altitude or density into log pressure. This is then used in the solution of the other fields

9. FINDROOT
   This routine uses a Newton-Raphson method to obtain pressure at a given altitude or density.

10. BVALU2
    This is a special version of the spline synthesis routine BVALUE that includes storm and IMF changes the altitude of the pressure surfaces.

11. ALTTR

Using the log pressure obtained in ALTTR1, ALTTR2 performs vertical transformations on each variable and for each spatial spectral coefficient m and n, and reduces B-spline coefficients to a single value. If the requested altitude is above the highest pressure surface, ALTTR2 assumes that winds and temperatures have reached their asymptotic values and assigns the appropriate variables.

12. SPACTR
Performs spherical harmonic synthesis at the requested latitude and longitude for each variable. For winds, it calls vector spherical harmonics V and W and for other variables, calls the scalar spherical harmonic P.

13. DIVTRAN
Performs the spherical harmonic synthesis for a non-rotational field.

14. ROTTRAN
Performs the spherical harmonic synthesis for a non-divergent vector field.

15. SCATRAN
Performs the spherical harmonic synthesis for a scalar field.

16. IONELEC
Corrects ion drift results.

17. DENSITY
Derives densities O, N_2, and O_2, and N mixing ratios.

18. RUNPARAM
This subroutine obtains necessary MSIS data to augment basic VSH model..

13. GETMSIS
Calls MSIS, if necessary, for high altitudes, low altitudes, and H densities.

Several additional calls are made in the time-dependent add-on parts of the model. They are listed in the following table.

Calls in STORM.

1. STORM
A driver routine that calls the subroutines that determine the storm difference fields.

2. STMCOEFFSEL
Selects coefficient files to be used in storm VSH and calculates the weights for these files.

3. STMCOEFFIN
Reads in the storm coefficient files required.

4. STMTIMESEL
Inputs correct coefficients for time.

5. STMBASIS
Determines components of the spherical harmonics as a function of longitude and latitude.

6. STMALTTR
Solves the spherical harmonics at the specific pressure corresponding to the altitude selected.

7. STMSPACTR

Calls routines that perform the synthesis of coefficients for the non-divergent field.

8. STMDIVTRAN
   Performs spatial synthesis of the coefficients for the non-rotational field.

9. STMROTTRAN
   Performs spatial synthesis of the coefficients for the non-divergent field.

10. STMSCATRAN
    Performs spatial synthesis of the coefficients for the scalar field.

11. STMREVTRAN
    Reads in geomagnetic-to-geographic conversion matrix for the scalar fields. Performs this conversion.

12. GTM
    Transformation of geographic location to a geomagnetic location.

13. MTG
    Transformation of a geomagnetic location to a geographic one.

14. TRANS_VEC
    Transforms geomagnetic vectors to geographic ones.

15. LATMAG
    Transforms geographic location into UT corrected geomagnetic location to acquire the storm coefficients at the correct place.

A further set of subroutine calls are mad in the IMF version of the model.

1. BYIMFX
   Sets up conditions if the Y component of the IMF is called

2. BYCOEFFSEL
   Selects coefficient files to be used and calculates weights for these files

3. BYCOEFFIN
   Reads in coefficients for the IMF cases

4. BYCORDSEL
   Matches the UT time with the By case and calls the routines to set up the geomagnetic coordinates

5. BYTIMESEL
   Transfers from one array to another to make the arrays compatible with a later subroutine.

PART III: TECHNICAL REFERENCE

CHAPTER 5: TIGCM RUNS

1 *Description*

The VSH model is based on the output from a set of runs of the NCAR Thermospheric-Ionospheric General Circulation Model (TIGCM). This model is run on a Cray supercomputer in Boulder, Colorado. The TIGCM solves the three-dimensional Navier-Stokes equations of fluid dynamics at each time step. Grid points are defined every 5 degrees in latitude and longitude and every half scale height in altitude. A time step of about 5 minutes is generally used.

The particular geophysical conditions chosen for the TIGCM runs are representative of the wide range of conditions that are experienced in the upper atmosphere. As additional runs of the model become available, the new data can be easily inserted as new libraries of coefficients in the VSH model.

Currently, 57 sets of coefficients from the TIGCM are available. There is a basic set of 18 runs (#21-38) that represent 3 different levels of magnetic activity (Ap), 3 days within the year (Julian days) representing seasonal variations, and 2 levels of solar activity (F10.7A and F10.7). The runs are summarized below.

In the table describing RUNS# 21 - 38, the first number in a number pair represents a RUN# for solar minimum (low F10.7); the second number is the RUN# for solar maximum (high F10.7). As an example, the run corresponding to a low F10.7A and F10.7, an AP of 11, and the December solstice is RUN #34.

RUNS #21 - 38

	EQUINOX	JUNE SOLSTICE	DECEMBER SOLSTICE
Ap			
5	21,24	27,30	33,36
11	22,25	28,31	34,37
32	23,26	29,32	35,38

In addition to the basic 18 runs (#21-38), there is an optional set of 23 additional runs that can be manually selected by the user. These additional runs are not normally included with the VSH package, but are available upon request. RUNS #1-17 represent the annual variation for AP=5 at both solar minimum solar maximum. RUNS #39-41 represent seasonal variations at middle values of the solar cycle. RUNS #42-44 represent the variation for the solar min-max Fritz peak study. In addition there are 8 sets of storm quiet difference coefficient files and the same number of IMF difference files.

In the standard vsh distribution there are 3*13 coefficient files, each representing a different variable (refer to chapter 5). Each of the main coefficient files contain fits to the basic set of runs 21 through 38. The other two sets contain the storm and IMF difference files.

2 *Density modification*

The mass density outputs from the TIGCM were found to require further adjustments to bring their values in line with climatologically averaged satellite data. This step is needed because the TIGCM is quite effective in capturing the density variations about a global mean, but less successful in computing the actual mean value. Therefore, for each run, at each pressure level, a mid-latitude comparison was made between the TIGCM and MSIS mass density. This difference between MSIS and VSH averages at each pressure level are used to correct VSH average presure level splines (refer to chapter 8). In this way altitudes are mapped to more reasonable pressure levels, enhancing VSH preformance for mass density calculations (as well as for other output variables).

The normalization (correction) factors are contained in the file HTMOD.DAT. Each row in this file contains the correction factors for each TIGCM run. The first column is the run number followed by the corrections to the seven average pressure level splines.

Similar to the normalization to MSIS values, density values from the SETA 2 satellite further normalize TIGCM average pressure versus altitude splines. The normalization (correction) factors are contained in the files SETAMOD.DAT. Each row in this file contains the correction factors for each TIGCM run. The first column is the run number followed by the corrections to the seven average pressure level splines.

CHAPTER 6: INTERPOLATION METHODS

The VSH model can produce composition and wind data for a wide range of geophysical conditions and for any location and time. The heart of the VSH model is its library of spectral coefficients. The coefficient libraries are obtained by applying spectral fits to the output fields from TIGCM runs. Using these libraries, VSH performs the inverse operation of synthesizing the desired fields from the spectral coefficients.

The spectral fit consists of the fitting of smooth curves to represent the variation of any output variable (such as mass mixing ratio or temperature) with respect to any input variable (such as latitude or ap). Each input/output relation is defined by 1) identifying a familiar, easily computable, family of curves (the basis functions) and 2) determining the best fitting linear combination of the basis functions to represent the actual atmospheric variations. Familiar examples of basis functions include the cosine and sine functions in a Fourier fit, and the polynomial functions in a least-squares fit. The weights that make up the linear combination of the fit - the spectral coefficients - are what is actually stored in the coefficient libraries.

This process of fitting spectral coefficients on the Cray, then reconstituting them in VSH, has two important features associated with it. First, the series generating the spectral coefficients are truncated at levels that reduce the computer storage requirements but retain the important variations of the output fields. In this way, computers of modest storage capabilities can take advantage of the results of a general circulation model over a wide range of geophysical conditions.

The second feature of this process is that a model based on discrete grid points, discrete times, and discrete geophysical conditions is converted into a model that is continuous over these same variables. The nature of the interpolation over each of its continuous domains is described in the following sections. It should be pointed out that some of the interpolations (such as the variation over solar activity) are actually carried out across several TIGCM runs (rather than within a run).

1 *Horizontal*

On a sphere, the spherical harmonics are the most natural basis functions to describe the latitudinal and longitudinal variations of a scalar variable. The spherical harmonics are represented mathematically as

$$Y_n^m(\theta,\lambda) = P_n^m(\cos\theta)\, e^{im\lambda} \qquad (8.1)$$

where the functions P are the Legendre polynomials, q is colatitude, and l is longitude. The value of a scalar quantity (e.g. mass density or temperature) at a particular location is calculated in VSH from the sum:

$$q(\theta,\lambda) = \sum_{m,n} a_{m,n}\, Y_n^m(\theta,\lambda) \qquad (8.2)$$

The coefficients $a_{m,n}$ are complex quantities because of the multiplication by e^{iml}. That is, the real part of $a_{m,n}$ will be multiplied by cos ml and the imaginary part will be multiplied by sin ml.

Despite the complicated mathematical form of the spherical harmonics, these functions are well understood and their values are easily calculated. The need for this level of sophistication arises because of the convergence of the longitudinal lines at the poles (where singularities can occur). The use of spherical harmonics allow the output fields to retain continuity across the poles.

For vector variables, a further consideration is required. The coordinate system is singular at the poles, because north and south wind directions are not continuous at the poles. A change of coordinates is carried out by expressing the wind as the sum of a gradient with zero curl (the velocity potential x) and a curl with zero gradient (the streamfunction y). That is, the horizontal wind field can be given as

$$\vec{U}(\theta,\lambda) = \nabla\xi(\theta,\lambda) + \nabla \times \vec{k}\,\psi(\theta,\lambda) \qquad (8.3)$$

In spherical coordinates, this vector equation is equivalent to the set

$$u(\theta,\lambda) = \frac{1}{r \sin\theta}\frac{\partial \xi}{\partial \lambda} + \frac{1}{r}\frac{\partial \psi}{\partial \theta}$$
$$v(\theta,\lambda) = -\frac{1}{r}\frac{\partial \xi}{\partial \theta} + \frac{1}{r \sin\theta}\frac{\partial \psi}{\partial \lambda} \qquad (8.4)$$

where r is the radius of the earth.

The velocity potential x and the streamfunction y are scalar variables that can be represented as sums of spherical harmonics using (8.1) and (8.2):

$$\xi(\theta,\lambda) = r \sum_{m,n} b_{m,n} Y_n^m(\theta,\lambda)$$
$$\psi(\theta,\lambda) = r \sum_{m,n} c_{m,n} Y_n^m(\theta,\lambda) \qquad (8.5)$$

(The radius of the earth r is introduced as a normalization factor.) Using the identities

$$\frac{\partial Y}{\partial \theta} = \frac{\partial P}{\partial \theta} e^{im\lambda} \qquad \frac{\partial Y}{\partial \lambda} = im P e^{im\lambda} \qquad (8.6)$$

and inserting (8.5) and (8.6) into (8.4): yields the formula for recreating winds from vector spherical harmonic coefficients $b_{m,n}$, $c_{m,n}$:

$$\begin{bmatrix} u \\ v \end{bmatrix} = \sum_{m,n} \left\{ b_{m,n} \begin{bmatrix} \frac{im P}{\sin\theta} \\ \frac{-\partial P}{\partial \theta} \end{bmatrix} + c_{m,n} \begin{bmatrix} \frac{\partial P}{\partial \theta} \\ \frac{im P}{\sin\theta} \end{bmatrix} \right\} e^{im\lambda} \qquad (8.7)$$

The distinction between scalar variables (such as temperature or density) and vector variables (such as neutral wind) is summarized in the table below.

Variable	Basis
Scalars	$P_n^n e^{im\lambda}$
Vectors	$\frac{m P}{\sin\theta} e^{im\lambda}$, $\frac{\partial P}{\partial \theta} e^{im\lambda}$

That is, scalars use a scalar basis function, while vectors use a vector basis. The functions

$$P_n^m \quad , \quad \frac{m P_n^m}{\sin\theta} \quad , \text{ and } \quad \frac{\partial P_n^m}{\partial \theta}$$

are precomputed.

The coefficient values, b and c, that go into the libraries were computed by performing a least-squares fit to minimize the squared error in the spectral representation. The algorithm for performing the least-squares fit is described in Schwarztrauber (1981). The actual values of the streamfunction and velocity potential are normalized by a division by $\sqrt{n(n+1)}$ where n is the meridional index.

2 *Vertical*

The vertical structure of a geophysical field is described by the least squares fit of a spline (a piecewise polynomial). A spline of degree n is defined as a piecewise polynomial of degree n, for which each of the first n-1 derivatives is continuous. Therefore, a cubic spline is a function that is continuous and for which its first two derivatives are continuous. The coefficients that define the cubic will generally vary from one subinterval to another.

The motivation for the use of splines to represent vertical variations, is that different physical processes occur at different altitudes. As a result, some variables may have very different vertical profiles in the vicinity of 100 km when compared to near 600 km.

In the TIGCM, the vertical variable is log pressure rather than geometric height. Therefore, the vertical representation of each of the dependent variables is carried out as a function of log pressure. Geometric height is also a dependent variable (as a function of log pressure) with its own set of coefficients in the coefficient library. Therefore, when a VSH user inputs an altitude, the spline defining altitude versus log pressure is inverted to convert the altitude to a log pressure. This log pressure can then be used to retrieve any of the desired output fields. The inversion of the altitude spline is carried out via a Newton-Raphson method of finding real roots.

In VSH, cubic splines are used in the altitude range of 110-500 km. Above about 500 km, the MSIS model is called. The 110-500 km range is divided into several subintervals. The polynomial has different coefficients in each of the subintervals. Each end point of the subinterval is known as a knot.

3 *Temporal*

With the exception of several experimental storm-time runs, the TIGCM produces diurnally reproducible results. At every hour of model time, the spherical harmonic fit described above is performed. The purpose of the temporal representation is to capture the variations of the spherical harmonic coefficients over the course of a day. A Fourier time series is used for this purpose.

A Fourier representation implicitly assumes that the output fields are periodic; that is, it is assumed that the fields reproduce themselves on a daily basis. This assumption is not valid during times of transient magnetic storm activity. The storm subset of VSH does not perform a spectral fit over the course of a magnetic storm, but instead records information for each hour of storm time.

The Fourier fit for the daily variation of any field is represented as follows:

$$a_{m,n,z} = \frac{a_{0,m,n,z}}{2} + \sum_{k=1}^{T} a_{k,m,n,z} \cos kt + \sum_{k=1}^{T} b_{k,m,n,z} \sin kt \qquad (8.8)$$

Seven coefficients are retained (T=3). This represents a constant term plus three (time) symmetric coefficients plus three (time) antisymmetric coefficients (diurnal, semidiurnal, and terdiurnal).

4. *Julian Day*

To account for the variations over the course of a year, the TIGCM is run under identical conditions at the two solstices and at an equinox. The solar annual cycle is described by a pure sinusoidal in radiation absorbed by the earth. In particular, the variations of any variable over the course of a year is currently fit using a two-point trigonometric interpolation. That is, a simple sinusoidal curve is assumed for both the annual and semiannual variations. Therefore, trigonometric interpolation between TIGCM runs is carried out. In future versions of the model, a Fourier fit over the annual cycle will be used as the TIGCM coefficient library fills up.

5. *Solar Flux*

Both of the solar flux arguments (F10.7 and F10.7a) influence the variation of most variables. F10.7a (the 90-day average) has the most bearing at lower altitudes. F10.7 expresses the daily transient flux, and becomes important at higher altitudes. These two parameters are synthesised into a single value of F10.7' using the relation:

$$F10.7' = F10.7a + k_1(h)*(F10.7-F10.7a) + k_2(h) * (F10.7 - F10.7a)^2$$

where h is height (or spline knot location), and $k_1(h)$ and $k_2(h)$ are weighting factors obtained from MSIS. The value of F10.7' is used for all subsequent calculation of geophysical fields. It is always found to be between F10.7 and F10.7a. Because the weights vary with height, the effecitive F10.7' value will also be height-dependent. As a result, different linear combinations of TIGCM runs may be used at different height levels. As anticipated, the k_1 factors increase monotonically with height. This reflects the increasing importance of daily solar activity with increasing height.

The $k_1(h)$ and $k_2(h)$ factors are contained within the file F107MOD.DAT. Each row in this file contains the linear (k_1) or quadratic (k_2) factors for each TIGCM run. The first column is the run number followed by the weighting factors for each height level.

6. *Magnetic Activity*

The variations over magnetic activity is carried out by a linear interpolation over Ap in the quiet time case. In the storm case, interpolation is made between Storm-quiet difference fields to provide an addition to a diurnally reproducible case (ap is set to 11 internally for the diurnally reproducible addition). For the scalar fields the difference coefficients are transformed mathematically and then the difference field is reconstituted and added to the quiet time output. The winds are treated differently because of the lack of a suitable algorithm for doing a transform on vector coefficients. The wind difference fields are reconstituted and then transformed to geographic coordinates. They are then added to the quiet time output.

7. *Variable Resolution*

A variable resolution scheme is used to improve the computational efficiency of VSH. The idea behind variable resolution is to process only those coefficients that will make a non-negligible contribution to the synthesis of the desired fields. In some instances, very few of the high order Fourier and spherical harmonic coefficients are required to capture important thermospheric properties.

VSH provides the user with a choice of five resolution levels. At the highest resolution, the model is most accurate but slowest. At lower resolutions, the model is faster, but less accurate. The availability of five resolution levels enable users to select appropriate spots on the performance-accuracy tradeoff curve. Generally speaking, the lower the resolution, the greater the smoothing that occurs within the model.

The resolution level is controlled by the FORTRAN variable IRES. The value of IRES has been preset to level 4, corresponding to nearly full resolution. By changing the value of IRES in the DATA statement, the resolution can be changed from 1 (lowest resolution) to 5 (highest resolution).

For each resolution level, there is i) a set of truncation levels for the spatial (or spherical harmonic) synthesis; ii) a set of truncation levels for the UT (or Fourier) syntheses, and iii) a set of difference thresholds. A difference threshold determines whether an input value is significantly different from that of the previous call. For example, a call to VSH with UT=12 followed by a call with UT=12.01 will not invoke a new synthesis of the Fourier time representation. For low resolution, the spherical harmonic and Fourier syntheses are highly truncated and the difference thresholds are set relatively high. For high

resolution, the Fourier syntheses extend through much higher values of m, n, and t in equations (8.7) and (8.8) and the difference thresholds are lower.

Associated with each of the five resolution levels is an error threshold value. Each error value represents the average deviation from the full resolution value. Coefficients that if excluded, would contribute an error exceeding the threshold are marked for retention. Any unmarked coefficients are unused in the synthesis, producing computational savings.

CHAPTER 7: OBJECTIVE ANALYSIS SCHEMES

1. *Density*

VSH allows the user to enter real-time satellite data to further improve upon its accuracy. The model has also been tuned to the climatological values of winds and density that have been accumulated over many satellite passes.

Some coefficient files will contain density modifications based on several passes of the SETA satellite. The slope and intercept used in the vertical representation of density will be modified so that their simulated global averages correspond to the observed satellite global averages. (also refer to chap. 7

2. *Winds*

Where available, Dynamics Explorer (DE) wind measurement data have been merged with the TIGCM simulation results. The merging process has been accomplished with techniques of objective analysis (Thiebaux and Pedder, 1987) that are commonly applied in meteorological analysis. In using objective analysis, a value of a field at a given grid point is computed from a weighted average of its computed TIGCM value there and observed values in a neighborhood of that location. The magnitude of the weight is inversely proportional to the distance of an observation from its site of prediction. In this manner, the winds contained in several coefficient sets actually consist of a background TIGCM wind field as modified by observations.

PART IV: SYSTEMS ANALYST'S REFERENCE

CHAPTER 8: INSTALLING VSH

1 *Program and library information*

The VSH model consists of two components: a set of FORTRAN subroutines and a library of numerical coefficients. The model is provided on a standard magnetic tape. It has been saved using the VAX/VMS BACKUP command with the volume identifier VSH and the save set name of VSH.BCK.

The FORTRAN subroutines are VSH, STORM, VSHIMF, VSHLIB, MSIS and SAMPLE. VSH contains the primary subroutines of the package, while VSHLIB contains the mathematical libraries. MSIS is a stand-alone atmospheric model that is called when the altitude is out of range of the values contained within the coefficient libraries. A sample main program SAMPLE is also included as a demo.

The numerical coefficient libraries are available in two versions. The VAX/VMS version contains the library coefficients already in the necessary binary unformatted form. In the non-VAX version, the coefficients are stored in ASCII unformatted form. Each coefficient file is named VARXX.YYY, where XX is a two-digit integer and YYY is either ASC (for ASCII files) or BIN (for binary files). The non-VAX version is further described in the following section.

The VAX version is immediately usable, once the files are transferred from tape to your computer.

2 *Use on a non-VAX machine*

The non-VAX version of VSH contains the coefficient library stored in ASCII format. A generic conversion program is included with this version to convert the ASCII files into binary. This program is named VAR_ASCTOBIN. Running VAR_ASCTOBIN will convert each VARXX.ASC file to a VARXX.BIN.

The FORTRAN subroutines VSH.FOR, VSHLIB.FOR, MSIS.FOR, and SAMPLE.FOR should be recompiled on the machine to be used. In addition, non-VAX users may need to change the name of two functions that are intrinsic to the VAX. These two functions convert characters to integers (CHAR) and real variables to integers (NINT). These two functions may appear in VSH, VSHLIB, ASCTOBIN and BINTOASC.

CHAPTER 9: STORAGE REQUIREMENTS

1 *Description*

The storage requirement on disk is essentially determined by the size of the coefficient files. These files are about 360K- 700K each in binary form for the basic runs. If you requested the files in ASCII form (for use on a non-VAX machine), the ASCII files will be found to be about three times larger than these values.

A breakdown of the storage requirements is the following:

vsh3by.f	79314 kB
storm.f	49198 kB
vshimf.f	23550 kB
vshlib.f	36035 kB
msis.f	50108 kB
gws3.f	19703 kB

and the coefficient files:

var01->var13	5888304 kB
stvar01->stvar13	8959520 kB
byvar01->byvar13	672256 kB

These values are for the sun UNIX system.

REFERENCES

Dickinson, R. E., E. C. Ridley, and R. G. Roble (1981) A three-dimensional general circulation model of the thermosphere, J. Geophys. Res., 86, 1499.

Hedin, A. E. (1987) MSIS-86 Thermospheric Model, J. Geophys. Res., 92, 4649.

Killeen, T. L., R. G. Roble, and N. W. Spencer (1987) A computer model of global thermospheric winds and temperatures, Adv. Space Res., 7, 207-215.

Swarztrauber R.N. (1981) The approximation of vector functions and their derivatives on the sphere, SIAM J. Numer. Anal., 18, 934-949.

Thiebaux, H.J. and M.A. Pedder (1987) Spatial Objective Analysis, Academic Press, London, 295 pp.

CHANGES FROM VERSION 1

Date	*Change*
Mar. 1991	Four new variables have been added: electron density, O^+ number density, ion temperature, and O2 mixing ratio. O^+ number density and ion temperature are given in the coefficient files as the natural logarithm of their actual values.
Mar. 1991	The OUTPUT variable array has been increased to 25 from 14, to incorporate the new variables and to allow for future expansion.
Mar. 1991	The range of inputs for ap has been extended to (2-60). The range of inputs for F10.7 has been extended to (50-350).
Aug. 1991	F10.7a added as an input variable
Aug 1993	The model extension to 90 km has been validated. The storm version of VSH has been included and validated for neutral densities and winds. Extra difference variable files are added. The IMF version is included in the package, but is switched off because no field has been validated. Extra difference fields are added.

14. Appendix 2.

Task Report on tasks 1, 2, and 3.

Nine tasks were listed in the three year period of this grant. It is the first three of these tasks that are of relevance here. These tasks are:

1) Update the current quiet-time coefficient files to include representations of runs made using NCAR-TIEGCM (National Center for Atmospheric Research - Thermosphere-Ionosphere-Electrodynamic General Circulation Model) rather than the NCAR-TIGCM (Thermosphere/Ionosphere GCM) runs that had previously been used.

2) The temperature representation in the VSH model will be revised to allow the vertical temperature structure to be determined without the use of Bates profiles.

3) Comparisons will be made between the present storm-time version of the model and data from storm-time orbits of the DE 2 (Dynamics Explorer 2) and AE (Atmosphere Explorer - C, D, and E) satellites.

Tasks 1, 2 and 3 were completed. The NCAR-TIEGCM was run for all of the appropriate conditions. However in doing this several problems were encountered during solar maximum conditions. It was found that the model was highly sensitive in these conditions and broke down. Upon creating coefficient files for these runs, it was found that the performance of the NCAR-TIEGCM was at this stage worse than that of the NCAR-TIGCM, so in consultation with the Technical Officer it was decided that the model was more reliable if it used the old files.

The temperature fields in the model were revised to allow a more correct vertical temperature structure to be included. This for the first time has permitted the model to calculate accurate storm-time temperatures.

Extensive comparisons were made between the storm versions of the model and data from the DE and AE satellites. The results are presented in the Technical report. Because of these comparisons corrections have been made to the VSH model. These changes are included in the delivered model.

Task Report on tasks 4, 5, and 6.

Nine tasks were listed in the three year period of this grant. It is the second three of these tasks that are of relevance here. These tasks are:

4) Further checks will made to assess the importance of the Y component of the Interplanetary Magnetic Field on the neutral winds, temperatures, composition and densities. A final decision will be made as to whether the gains made in terms of accuracy are more important than the losses due to reduced efficiency.

5) The importance of variations of the Y component of the IMF during storms will be assessed. Changes in the Y component during these times are likely to be more important than changes during quiet geomagnetic times , so this separate study is necessary.

6) If needed, the effects of the Y-component if the IMF on the neutral thermosphere during geomagnetic storms will be included in the VSH model.

During the PI's visit to Marshall in November the Technical Officer (Jeff Anderson) stated during discussions that the work relating to IMF effects in the VSH model were not of great interest to the Scientific and Technical Staff at Marshall because their main problems involved the prediction of thermospheric effects on satellite's in low inclination orbit. Instead the Technical Officer (Jeff Anderson) stated that the Staff at Marshall would be interested in a system of quick checks to be able to see what the historical densities were at a particular site that a satellite might travel through. He indicated that the PI should decrease the scope of tasks 4 through 6 without indicating how this was to be done. In addition the limitation of funds (only the first half of the second year's funds were ever allocated) prevented the employment of more staff to carry out the work. Despite this work was completed on tasks 4 through 6. It was found that the IMF effects

on composition and neutral densities were not of sufficient importance (being restricted to high latitudes) to the mission of Marshall to be included in the model. The main reasons for not including these effects are: they are relatively unimportant (see the technical report); and that a far greater computer overhead would result from their inclusion.

PREFACE

This manual is divided into four sections. Part I provides an overview of the capabilities of VSH. This part is oriented towards all users of VSH and provides the minimum information needed by an end user. Part II details how a FORTRAN program would be written to access the VSH routines. It includes examples of main programs. Part III is a technical description of the underlying atmospheric physics and mathematical equations used in the VSH model. It is most useful for space scientists and others who are interested in the underlying science that went into the development of the VSH model. The final section is directed towards a systems analyst or systems administrator. It provides information on storage, run-time requirements, and installation.